Infrared Spectroscopy of Size-Selected Water and Methanol Clusters

Udo Buck* and Friedrich Huisken†

Max-Planck-Institut für Strömungsforschung, Bunsenstrasse 10, D-37073 Göttingen, Germany

Received February 3, 2000

Contents

I. Introduction

The investigation of structural and dynamical properties of weakly bound clusters has attracted a great deal of interest in recent years.[1−5] They provide an exceptional tool to study the microscopic behavior of a number of macroscopic phenomena which are important in physics and chemistry. The advantage of clusters is the possibility to simply vary the size and to investigate the development of properties of the condensed phase step by step which are otherwise difficult to disentangle. In addition, the finite number of particles in a well-defined environment helps to determine the theoretical concepts, which are easier to carry out than the direct treatment of bulk liquids and solids. Of special interest are the hydrogen-bonded clusters. These complex networks determine the usual and unusual properties of the most important solvent molecules such as alcohols and water. The latter one is of particular importance because of the role that water plays as ubiquitous solvent and that ice particles have in atmospheric and extraterrestrial physics and chemistry. For these OH-containing systems, the measurement of the OH stretch vibration by infrared spectroscopy has proved to be a very sensitive indicator of the strength of the hydrogen bond. Therefore, it is not surprising that this method has also been widely applied for the investigation of clusters. In particular, these studies include direct absorption experiments with infrared[6] and far-infrared excitation,[7,8] the cavity-ring-down method,[9] and the optothermal detection,[10−13] in which the positive (excitation) or negative (dissociation) energy content of the beam is detected by a low-temperature bolometer. All these methods, however, work best for the small complexes when the spectra do not overlap. In favorable cases, the spectra themselves can be used to identify the cluster size based on accompanying calculations.

In general, however, the identification has to be carried out by measurements which are size-selective. This is not a simple task since the techniques for generating free cluster beams, the supersonic adiabatic expansion or the aggregation in cold gas flows, produce in almost all cases a distribution of cluster sizes.[14] In principle, the problem could be solved by a size-specific detection method. The most commonly used detection method, the ionization and the subsequent mass selection in a mass spectrometer, is hampered by fragmentation during the ionization process. It is caused by the energy released into the system as the clusters change from their neutral to their ionic equilibrium structure. This excess energy then leads to the evaporation of neutral subunits, and thus, fragmentation occurs.[15,16] For the molecular species considered here, the resulting fragmentation pattern is often modified by fast chemical reactions of one of the ionized molecular units with neutral partner molecules within the cluster.[16,17] In any case, a simple mass spectrum does not characterize the neutral cluster distribution at all.

Therefore, selection methods have to be applied to make sure that the experiments are carried out with one neutral cluster size only. One possibility is to use

* To whom correspondence should be addressed. Telephone: +49-551-5176-572. Fax: +49-551-5176-607. E-mail: ubuck@gwdg.de.
† E-mail: fhuiske@gwdg.de.

10.1021/cr990054v CCC: $35.00
Published on Web 09/23/2000

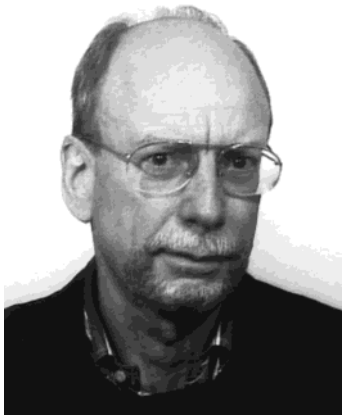

Udo Buck was born in 1938 in Kamen/Westfalen, Germany, where he also attended high school. In 1958 he went to the University of Göttingen and Bonn to study physics. He received his Diploma in Physics in 1965 in the institute of W. Paul and his Doctor of Science in 1969 under the supervision of H. Pauly at the University of Bonn. The topic of his thesis was the direct inversion of high-resolution differential cross sections obtained in crossed molecular beams to the interaction potential. Then he joined the Max-Planck-Institut für Strömungsforschung in Göttingen to continue the research on elastic and preferentially rotationally inelastic molecular scattering processes and the determination of the anisotropic interaction. In 1971 he was a visiting scientist at the University of Genua, Italy, with G. Scoles. In 1976 he was appointed Associated Research Fellow at the Max-Planck-Institut and in 1980 Professor of Physics at the University of Göttingen. His research interest gradually moved to the investigation of the spectroscopy and the dynamics of size-selected clusters with emphasis on hydrogen-bonded systems. He was a visiting professor at the Australian National University, the University of Washington, and, several times, the University of California, Irvine. In 1991 he received the Max-Planck Research Award.

Friedrich Huisken was born in Rheinberg/Rhld, Germany, in 1946. He attended high school in Rheinberg and, after military service, went to Göttingen to study physics. After receiving his Diploma in 1973, he began his Ph.D. work at the Max-Planck-Institut für Strömungsforschung under the direction of Professor H. Pauly and Professor U. Buck and carried out experiments devoted to the rotational excitation of hydrogen molecules in crossed molecular beams. He obtained his Ph.D. degree in 1978. After a one-year stay with Professor Y. T. Lee at the Lawrence Berkeley National Laboratory, where he studied the mulitphoton excitation and dissociation of molecules and clusters, he returned to the Max-Planck-Institut für Strömungsforschung to establish his own research group. In the following years he carried out experiments to study the spectroscopy of van der Waals and hydrogen-bonded clusters using nonlinear Raman techniques and infrared spectroscopy. In 1990 he habilitated at the University of Göttingen with a thesis on the vibrational spectroscopy of size-selected molecular clusters. Since 1996 he as been Associate Professor at the Physics Department of the University of Göttingen. His current research focuses on the spectroscopic investigation of molecules and complexes trapped in liquid helium clusters and the study of light-emitting silicon nanoparticles.

special ionization techniques for a certain class of molecules. A well-known example is the two-color resonant two-photon ionization of aromatic molecules.[18,19] In this case, the neutral and ionic equilibrium structures are similar and, by carefully adjusting the ionization energy near the threshold region, the fragmentation is avoided. In addition, the first step, the excitation of a suitable electronic state, can be made size-specific so that a very reliable method results. This is, however, restricted to molecules with suitable electronic transitions, and the chromophore molecule is always present as a perturber. Applications for water- and methanol-containing systems are available for benzene−water,[20,21] phenol−water,[22−25] and some other substituted benzene−water systems[26] as well as for benzene−methanol[27,28] clusters.

Another method is the *momentum transfer* in a scattering experiment with atoms. In a high-resolution crossed beam arrangement, the clusters are separated from each other by making use of their different angular and velocity distributions in a single collision experiment.[29,30,16,17] Because of the resolution requirements, this method is restricted to sizes $n \leq 15$. Results obtained by this method will be the main topic of this article. We note that the *high-resolution spectrum* itself has been used as a fingerprint of the cluster size in the rotation−vibrational−tunneling spectroscopy of water clusters using far-infrared laser absorption.[31−33] The largest size analyzed in this way is $n = 6$.

Thus, it is the main purpose of this article to summarize our recent studies on the structure and dynamics of molecular clusters of the type ROH (R = H, CH_3) using the scattering method for the preparation of clusters of one size and combining it with infrared photodissociation spectroscopy. The selection method is followed by an appreciable loss of intensity, and thus, certain restrictions in the experimental variety occur. However, by applying this technique, we have the great advantage that we definitely know that we measure the spectrum of one size only. The questions we would like to answer include the following: (1) How can the spectrum, characterized by the line shifts, be related to the structure of the clusters? (2) What is the role that different isomers play, and how does their existence depend on the temperature? (3) What is the dependence on cluster size and, if available, on the excited mode? (4) Are there differences for free and embedded or adsorbed clusters, and what are the reasons for it? (5) How do the different systems compare with each other?

Detailed results will be presented for the two prototype systems of the ROH type with a nearly linear hydrogen bond H_2O and CH_3OH. For pure water clusters, results are available up to $n = 10$. In addition, small clusters have also been investigated in large helium droplets and on medium-sized argon clusters. Similar results are available for methanol. Here, both the OH stretch and the CO stretch were studied, and also mixed clusters of water and methanol will be considered.

The article starts with a short description of the experimental tools, the size selection, the infrared

photodissociation, and the different methods to generate clusters absorbed on the surface or embedded in the interior of a large cluster. In the main part of this paper, we will present the results and try to answer the questions listed earlier. In addition, we will compare the results with those obtained for the condensed phase and for clusters using different experimental methods.

We will also include results which are either not size-selected or are perturbed by chromophore molecules. Finally, we will discuss the structure and the existence of isomers of this important group of clusters. We will essentially cover the results of the last 5 years. Several articles and reviews on the spectroscopy of size-selected molecular clusters have already appeared. Some of them are relatively short contributions to conferences[34−42] which also address other subjects. Others deal only with a certain aspect of the field or do not contain the latest results which have been obtained both in the interpretation of the measured infrared spectra and in terms of new experimental results.[43−47] The last detailed and comprehensive reviews[48,49] appeared some years ago. We note that results for other hydrogen-bonded systems obtained with size-selected clusters which are not treated here are available for ammonia (NH_3),[50,51] hydrazine (N_2H_4),[52,46] acetonitrile (CH_3CN),[45,53] hydrogen fluoride (HF),[54,55] methyl fluoride (CH_3F),[56] and ethanol (C_2H_5OH).[57]

II. Experimental Methods

A. Size Selection

The method of size selection by momentum transfer in a scattering experiment with atoms under single-collision conditions has been described in detail in the literature;[29,16,30,36,48] thus, we give here only a short account of the principle. The method is based on the fact that the heavier clusters are scattered into smaller angular ranges with different final velocities compared to the lighter clusters. For elastic scattering, all final center-of-mass (cm) velocities $u_c^{(n)}$ of the clusters of size n are restricted to end on a sphere around the center-of-mass with the radius

$$u_c^{(n)} = m_d g/(n m_1 + m_d) \qquad (1)$$

where m_d is the mass of the deflecting beam, m_1 the monomer mass of the cluster of the size n, and g the relative velocity. In the case of inelastic scattering, one has to take into account the transferred energy ΔE which changes the final velocity according to $u_c' = u_c(1 - \Delta E/E)^{1/2}$, where E is the collision energy. Since, before collision, the different clusters have nearly the same velocity v_c in the laboratory system (lab), their relative velocities g are also nearly independent of the cluster size while the final cm velocities $u_c^{(n)}$ are quite different. With increasing mass of the clusters, they decrease and so do the radii of the spheres and thus the maximum lab deflection angles. It is immediately clear from this picture that larger clusters can easily be excluded by choosing the correct *angle* for detection. For the necessary additional discrimination against smaller clusters, two solutions are used, the measurement of the velocity or the measurement of the mass.[30,16,17]

In the first method, in addition to the angle, the final *velocity* is specified. For this purpose, either time-of-flight analysis or a mechanical velocity selector[58] is used. This procedure is general and completely independent of the subsequent detection process. In the second method, a *mass* spectrometer is used to discriminate against the smaller clusters. This method is applied for the size selection of the molecular clusters discussed here. The procedure works best if at least a small fraction of the cluster M_n is detected at the nominal mass of the ion M_n^+ or at a fragment mass M_k^+ which is larger than that of the next smaller cluster M_{n-1}^+. Clusters of the $(ROH)_n$ type are very often detected at the mass of the protonated ion $(ROH)_{n-1}H^+$ of the next smaller cluster.

The procedure requires, in general, a high-resolution molecular beam apparatus and intense cluster beams with good expansion conditions to minimize the angular ($\Delta\Theta < 0.1°$) and velocity spread ($\Delta v/v < 0.05$) of the colliding beams. The first part is realized by skimmed beams introducing additional apertures. The latter is usually achieved by expanding a mixture of 2−10% of gas in helium or neon.

The natural limit of this procedure for size-selecting clusters is given by the fact that the maximum deflection angles for the different sizes come closer and closer together with increasing n. In our experimental arrangement, it is no problem to select clusters with $n = 6$ for monomer masses around $m_1 = 50$ u when He is used as scattering partner ($m_d = 4$ u). These values depend, however, very much on the masses and velocities of the particles. Increasing $m_c = n m_1$ and v_c deteriorates the resolution, while increasing m_d and v_d improves it. In the former case, the Newton spheres shrink, while in the latter case the contrary is valid. For the masses, this result follows directly from eq 1.

These considerations were recently demonstrated in experiments with acetonitrile, which was seeded in neon instead of helium, which decreases v_c. Scattering from Ne and Ar instead of He increases m_d in addition. At a lab scattering angle of 6°, cluster sizes of $n = 5$, 12, and 20 are detected for the scattering from He, Ne, and Ar, respectively. In this way, $(CH_3CN)_n$ clusters were selected up to $n = 24 \pm 3$.[36,45]

In general, the scattering process reduces the intensity by a factor of 10^6, so that a beam, which consists of one cluster size only, contains about 3×10^{12} particles per sr and s. It is noted that during the scattering process, a certain amount of energy is transferred into the cluster. This is especially valid if Ne or Ar is used as the scattering partner instead of He. This fact does not disturb the size selection. As already mentioned earlier, the radii of the spheres get smaller and the procedure works as with elastic scattering. The reason is 2-fold. First, the different cluster sizes are, in general, equally affected by the inelastic scattering, and thus, all the spheres become smaller by the same amount. Second, by selecting the deflecting angle for the detection close to the elastic

limit, the influence of the internal excitation can be reduced. In any case, this effect can be measured by time-of-flight analysis and taken into account in the data evaluation.

We also note that there is a remarkable influence of the collisional excitation on the width of the bands if measured after the size selection. For the CO stretch band in methanol dimers, values between 30.9 and 37.3 cm^{-1} were observed depending on the amount of energy put into the system.[59,60] For cold size-selected clusters (see section II.B), line widths around 4.0 cm^{-1} were measured,[61,62] while for a very dilute mixture of methanol in helium/neon, a value of 2.4 cm^{-1} was achieved.[63] For larger internally excited clusters, these values decrease from 13.3 cm^{-1} for the trimer, 8.5 cm^{-1} for the tetramer, 7.3 cm^{-1} for the pentamer, to 6.3 cm^{-1} for the hexamer.[60] Apparently the increasing number of degrees of freedom which are available for these clusters helps to distribute the energy so that the effect gradually disappears for larger clusters.

B. Molecular Beam Depletion Spectroscopy

The cluster absorption spectra are measured using a technique that exploits the collimation and directional properties of a molecular beam and the dissociative behavior of weakly bound complexes upon absorption of a single IR photon. This technique is termed molecular beam depletion spectroscopy. It was first proposed by Klemperer[64] and later experimentally realized by Gough, Miller, and Scoles.[11] In their experiment, Gough et al.[11] produced a molecular beam containing N_2O monomers and van der Waals (vdW) clusters. This beam was crossed by the radiation of a tunable IR laser and directed to a liquid-helium-cooled bolometer or, alternatively, to a mass spectrometer detector. Since the excitation energy (-2225 cm^{-1}) is larger than the cluster binding energy and since there is sufficient coupling between the excited intramolecular mode and the intermolecular vdW modes, every cluster excitation results in its prompt dissociation.[65] The fragments of the dissociated cluster are expelled from the cluster beam, and thus, the occurrence of dissociation or equivalently absorption is readily detected by monitoring the decrease in cluster signal. This technique constitutes an elegant and very sensitive alternative to the more direct absorption spectroscopy.

Shortly after its demonstration, the new technique was applied worldwide by several laboratories specialized in molecular beam studies. Pioneering work was carried out in the laboratories of Scoles,[11] Reuss,[66] and Watts[67] using a bolometer as the detector and Lee,[68] Janda,[69] Gentry,[70] and Klemperer[71] employing a mass spectrometer detector.

C. Molecular Beam Machines and Experimental Setups

The measurements were carried out in two different crossed molecular beam machines which have been described in several publications and which are referred to here as Apparatus I[60,72] and Apparatus II.[48,54,73,74] While in Apparatus I the deflection angle is varied by rotating the atom and cluster beam sources about the scattering center and keeping the detector stationary, in Apparatus II the beam sources are stationary and the detector is rotated about the scattering center. Both cluster beam machines make use of the size-selection technique discussed in the previous section. To combine the molecular beam depletion spectroscopy[46] and the cluster selection technique, two possible configurations arise: the clusters can be excited by the laser either before the scattering center or behind it. In Apparatus I, it is most convenient to direct the laser beam through the stationary detector so that it interacts with the scattered and size-selected clusters. In contrast, in Apparatus II where the detector is rotated, it is more appropriate to place the interaction of the clusters with the laser beam before the scattering center.

The different configurations used in the two cluster beam machines are schematically depicted in Figure 1. Each geometry has its own merit, and both configurations complement each other very nicely. The conceptionally simpler configuration is that of Apparatus I. Here the clusters are selected by the scattering process before they are probed by the laser. By choosing a deflection angle appropriate for selecting cluster size n, the laser beam will interact only with clusters of size $k \leq n$. If the quadrupole mass spectrometer is tuned to a mass larger than that of size $n - 1$, the depletion is monitored only for the clusters of size n. Since the laser is pulsed, the interaction with the scattered cluster beam results in a transient depletion signal which is measured by time-of-flight analysis as schematically shown in the inset of Figure 1. The depletion is measured for each laser frequency, and in this way a size-selected cluster spectrum is obtained. It has been discussed before that due to the scattering process, the selected clusters may be internally excited.

In Apparatus II (see Figure 1b), the laser always interacts with internally cold clusters as they were prepared by the adiabatic expansion. However, in contrast to the previous situation, it interacts with *all* clusters present in the beam. If the laser radiation is absorbed by the clusters of size n, they will be dissociated and the resulting depletion will also be translated to the scattered beam. Therefore, with the mass spectrometer tuned to the proper angle and mass, it is possible to measure a size-selected absorption spectrum just as is the case with Apparatus I, except that the addressed species are cold now. Unfortunately, this configuration has a serious drawback when larger clusters are to be studied since, in that case, we have to choose small deflection angles. If it now happens that at the same laser frequency larger clusters are also dissociated, the resulting fragments may be directed into the detector without being scattered. Thus, they give rise to a positive contribution to the signal which will interfere with the depletion signal carried by the scattered clusters of the proper size n. If these two contributions cannot be untangled, it is not possible to measure a proper absorption spectrum.

Summarizing the merits and drawbacks of the two different configurations, we can state that Apparatus

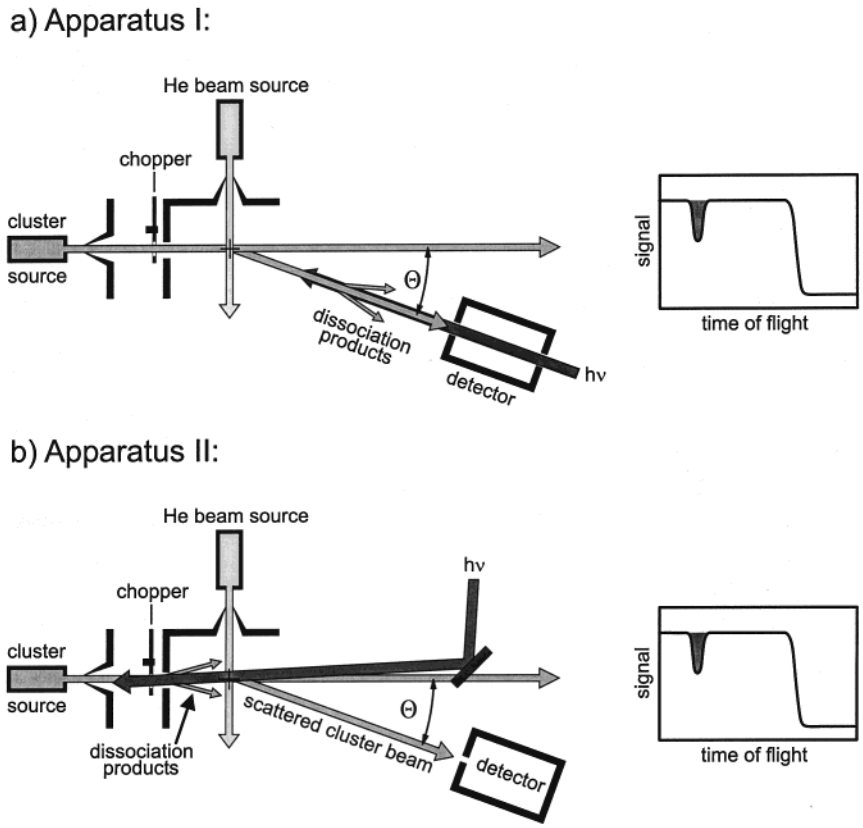

Figure 1. Schematic view of the experimental setups (Apparatus I and II) used for the present study. The main difference between the two configurations is that in Apparatus I the laser beam interacts with size-selected internally warm clusters while in Apparatus II the interaction takes place with the unselected beam of cold clusters. Apparatus II is more suitable for the spectroscopy of small clusters, whereas Apparatus I is superior for the study of larger species.

II will be more suitable for the study of smaller clusters ($n \leq 6$) while Apparatus I will be superior if larger clusters are to be investigated ($n \geq 5$). The appropriate cluster sizes given in parentheses are typical values which may depend on the system.

Due to the significantly reduced intensity of the scattered cluster beam, the size-selective studies are rather time-consuming. Therefore, it is often useful to first measure an overview spectrum in the direct nonselected cluster beam. Of course, all cluster sizes having absorption bands in the investigated spectral range will contribute to this spectrum. Such overview spectrum can be obtained in two different ways. It is possible to monitor the depletion in the nonselected beam, or it is equally possible to measure the signal enhancement produced when the dissociation products are deflected into the detector that should be positioned at a small scattering angle $\Theta \neq 0°$ (typically $2° \leq \Theta \leq 4°$). The latter technique is referred to as *fragment spectroscopy*. Both configurations are depicted in Figure 2. Whereas depletion spectroscopy in the direct beam may be hampered by a small signal on a large background, fragment spectroscopy has the advantage that the background is usually very low, especially if the deflection angle is chosen to be not too small. Depletion spectroscopy can be carried out in both molecular beam machines (Apparatus I and II); fragment spectroscopy, however, is reserved to Apparatus II. Even though both methods are not size-selective, some size-specific information is obtained from the setting of the mass spectrometer. Assume that the mass spectrometer is tuned to the mass of the cluster of size k. Then, in depletion (fragment) spectroscopy, all clusters with $n \geq k$ ($n \geq k + 1$) may contribute to the spectrum, provided that they absorb in the respective spectral range. By measuring the overview spectra with different settings of the mass spectrometer, it is, in some cases, possible to derive size-specific information just by comparing the different spectra. In some studies, we have applied an alternative procedure. It consists of first measuring an overview spectrum (in depletion or as a fragment spectrum) and then determining to what cluster size each absorption band belongs. The assignment is made by measuring, with the secondary beam on and the laser tuned to the maximum of the respective absorption band, the laser-induced depletion as a function of the deflection angle. In this way, it is possible to determine, from the cutoff angle, the cluster size responsible for the absorption band and to properly assign the various absorption bands measured in the overview spectrum.

The techniques just discussed are employed for the study of gas-phase clusters. Complementary information is obtained by attaching or embedding the hydrogen-bonded complexes $[(ROH)_n]$ to or in large rare-gas host clusters (Rg_N, Rg = He or Ar). The composite cluster systems, designated by $(ROH)_n \cdot Rg_N$, are generated by making use of the pickup technique introduced by Gough et al.[75] The experiments with argon clusters were carried out with the

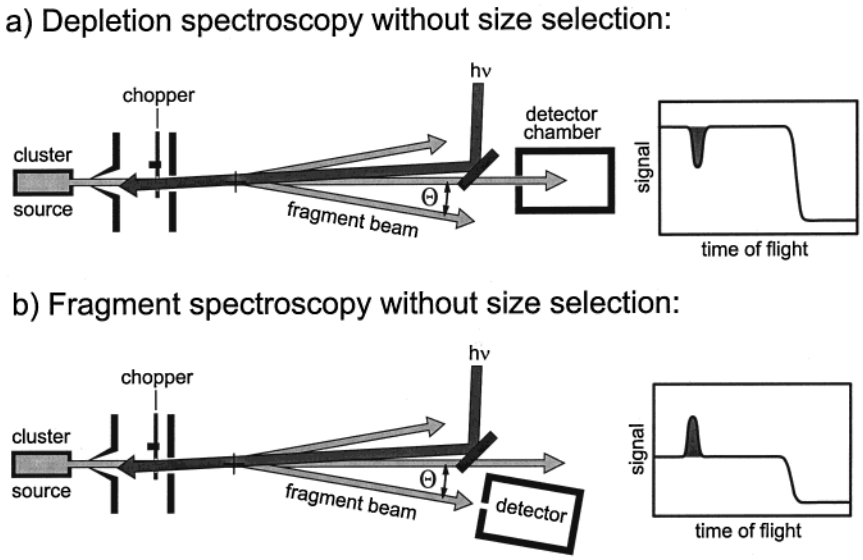

Figure 2. Two possible configurations used to measure an overview absorption spectrum without size selection. In the upper configuration, the laser-induced depletion is monitored with the detector positioned at $\Theta = 0°$. In configuration b, the detector is positioned off-axis ($2° \leq \Theta \leq 4°$) and the laser-induced dissociation products are measured as an increase in signal.

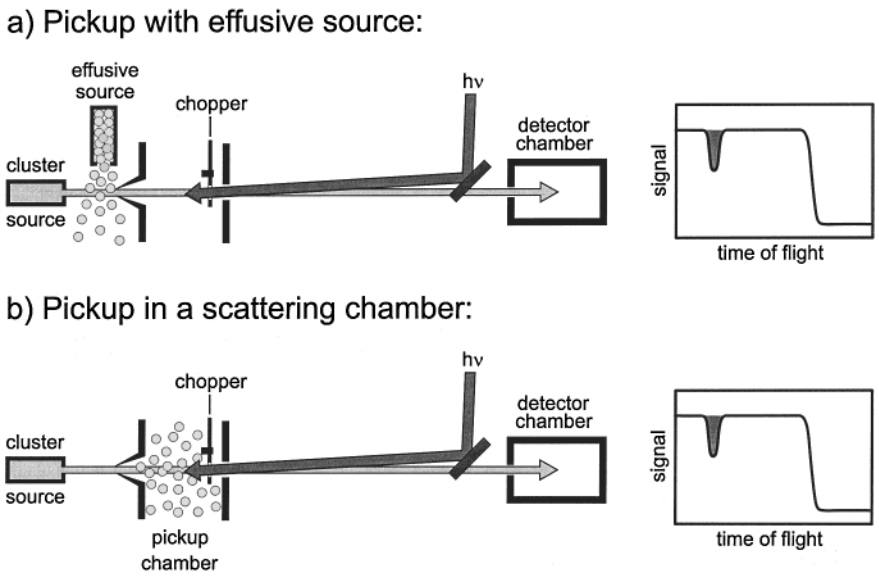

Figure 3. Schematic sketch of the experimental setups used for the IR spectroscopy of rare-gas clusters, Rg_N, doped with hydrogen-bonded complexes, $(ROH)_n$.

experimental arrangement shown in Figure 3a and described in more detail elsewhere.[73,76] Briefly, argon clusters (Ar_N) with an estimated mean size of $\langle N \rangle = 50$ are produced by expanding argon gas at high pressure into the vacuum. Before entering the differential chamber through the skimmer, the argon cluster beam is crossed by a beam of ROH molecules emanating from an effusive molecular beam source operated at stagnation pressures below 50 mbar. Upon collisions, monomeric ROH molecules are attached to the argon clusters and carried by them to the detector. At larger pickup source pressures, multiple adsorption occurs and, by interacting through their large dipole moment, the ROH molecules aggregate and form small polymers within or on the surface of the host clusters. The process follows a Poisson distribution with a simple correlation between the size of the complexes and the pressure of the chromophore molecules.[77] Due to the strong fragmentation of the composite clusters in the ionizer, the small ROH complexes can be detected on the typical fragmentation channels known from the mass spectrometry of gas-phase ROH polymers.[73] Unfortunately, the kinematic size-selection technique discussed before cannot be applied since the large argon clusters are too heavy to be sufficiently deflected by the helium beam.

When the embedded ROH complexes are excited by IR radiation, the vibrational energy is transferred to the host cluster which acts as a heat bath. The excess energy is rapidly released by evaporating ca. 10 Ar atoms. This evaporation leads to a broadening of the angular width of the cluster beam and to a reduction of the ionization cross section. Both effects

result in a depletion signal measured with the mass spectrometer as shown in the schematic time-of-flight spectrum of Figure 3a.

For the production of ROH complexes embedded in large helium clusters [$(ROH)_n \cdot He_N$], the setup has been slightly changed[74] (see Figure 3b). The helium cluster beam is generated by supersonic expansion of helium gas through a pinhole nozzle cooled with liquid helium to temperatures around $T_0 = 20$ K. At a stagnation pressure of $p_0 = 40$ bar, we produce helium clusters containing between 1000 and 6000 He atoms on the average. The helium clusters then pass through the differential chamber which serves as the pickup chamber. For this purpose it is filled with ROH vapor adjusted to the desired partial pressure of ca. 1×10^{-5} mbar.

The free ROH clusters were generated by expanding mixtures of 5−20% ROH in helium at total pressures of $p_0 = 2$ bar through pinhole or conical nozzles with diameters of 100 μm kept at temperatures between 273 and 373 K. After passing through a differential chamber, the skimmed and collimated ROH cluster beams could be crossed by a secondary helium beam if size-selective information was required. Finally, the scattered cluster species were detected by a stationary (Apparatus I) or rotatable (Apparatus II) mass spectrometer detector equipped with electron bombardment ionizer ($E = 100$ eV, $I =$ 15 mA), quadrupole mass filter, and electron multiplier. To produce the Ar (He) host clusters, we used a 50 (5) μm diameter pinhole nozzle, kept at 300 (18−24) K, and a backing pressure of 7.5 (40) bar.[73,74] These conditions resulted in mean cluster sizes of $\langle N \rangle = 50$ for Ar_N and 1000−5400 for He_N.

The infrared radiation used to excite and dissociate the clusters was obtained from either a CO_2 laser or a Nd:YAG laser-pumped optical parametric oscillator (OPO). To access the spectral region from 1000 to 1100 cm^{-1}, in which we could excite, besides some methyl rocking modes, the CO stretch of MeOH, either a cw (Apparatus I) or a pulsed (Apparatus II) CO_2 laser was used. The more recent experiments were carried out in the spectral region from 2800 to 3800 cm^{-1} in which we could address the CH stretch of MeOH and, most importantly, the OH stretches of all clusters discussed here. This infrared radiation was obtained from an injection-seeded OPO.[78] It consisted of a master oscillator containing a $LiNbO_3$ crystal, which was pumped by the fundamental of a Nd:YAG laser. The master oscillator was seeded by the narrow-bandwidth infrared radiation obtained by difference frequency mixing the output of a pulsed dye laser and the 532 nm radiation of the same Nd:YAG laser in a $LiIO_3$ crystal. The typical output energy for the low-frequency component (idler) was ≥4 mJ per pulse in the entire spectral range covered in this study. The bandwidth of the infrared radiation, $\Gamma = 0.25$ or 2 cm^{-1}, which was determined by the bandwidth of the dye laser, was chosen to be 2 cm^{-1} in most experiments carried out in Apparatus II. The bandwidth obtained in Apparatus I was 0.5 cm^{-1}.

The interaction between cluster and laser beams was realized by using a collinear configuration with counterpropagating laser beams (Apparatus I) or a quasicollinear configuration with the laser beam intersecting the cluster beam at small angles (Apparatus II). The absorption of the IR photons by the clusters and the following dissociation was monitored by observing either the reduction of the signal in the direct or scattered beams (depletion spectra) or the enhancement of the signal on a fragment mass with the detector positioned to a small deflection angle (fragment spectra). In each case, the signal was monitored in real-time, using a computer-controlled time-of-flight analyzer[79] triggered by the laser. To determine the dissociation yields quantitatively, the measured TOF spectra were convoluted taking into account the clusters' time-of-flight distributions.[48]

III. Water Clusters

A. Introduction

The exploration of the structural and binding properties of water clusters $(H_2O)_n$ provides a key instrument for the understanding of bulk water in its solid and liquid phase as well as for the understanding of the solvation properties of the most important solvent. At first, the highest priority was given to the theoretical and experimental study of small water complexes. In the meantime, the structure and dynamics of small water clusters ($n < 10$) are already quite well understood and emphasis is now being placed more and more on larger systems.

Early structural information on water polymers has been obtained from molecular beam electric deflection studies.[80] These experiments revealed the polar nature of the dimer, consistent with a linear hydrogen bond, and the nonpolar character of the higher polymers with $n = 3-6$, suggesting that the larger complexes have cyclic structures. These experimental results were predicted by early[81] ab initio calculations and have been confirmed by more recent[82−89] ab initio calculations.

The first vibrational studies of water clusters were devoted to the investigation of the intramolecular modes. The water monomer has three fundamental vibrations: the bending mode (ν_2) near 1595 cm^{-1}, the symmetric OH stretch[90] (ν_1) at 3657.05 cm^{-1}, and the asymmetric OH stretch[90] (ν_3) at 3755.97 cm^{-1}. In the water dimer which consists of two nonequivalent water molecules (the proton donor and proton acceptor), each vibration splits into two components. Correspondingly, larger $(H_2O)_n$ polymers have n components for each intramolecular vibration.[82,84] Due to the unfavorable wavelength around 6.3 μm needed to excite the ν_2 bending mode, this vibration has only been studied in matrix isolation experiments[91−94] and very recently also in cluster distributions using CRD and FTIR spectroscopy.[95,96] In contrast, it is easier to access the 2.7 μm region where the symmetric and asymmetric OH stretching vibrations can be excited using various continuous-wave lasers or pulsed laser sources in conjunction with nonlinear frequency conversion techniques.

The first absorption studies of the stretching vibrations of gas-phase water clusters were carried out by Lee and co-workers[97,68] employing molecular beam

vibrational predissociation spectroscopy with an optical parametric oscillator. Although the problem of fragmentation in the electron bombardment ionizer was realized and care was taken to minimize this effect, the broad spectra seemed to be strongly affected by the fragmentation of larger polymers. The following study, carried out by Page et al.[98] in the same laboratory, focused on the IR spectroscopy of the water dimer, $(H_2O)_2$. The four major absorption bands were assigned to the excitation of the symmetric (ν_1) and asymmetric (ν_3) stretching vibrations in the nonequivalent dimer constituents as discussed before. The most red-shifted band at $\tilde{\nu}_0 = 3545$ cm^{-1} was attributed to the donor ν_1 vibration, which, in later studies,[99] was associated with the stretching vibration of the OH group engaged in the hydrogen bond and is now referred to as the bonded OH stretch. Shortly after that, Coker et al.[99] studied the evolution of water polymer spectra from the dimer to large clusters employing their molecular beam color center laser apparatus with bolometric detection. At their mildest expansion conditions, they observed four absorption bands, in agreement with the earlier study of Page et al.[98] Again, the most red-shifted band (now at 3532 cm^{-1}) was attributed to the bonded OH stretch of the water dimer. The assignment of all four spectral features to the water dimer was strongly supported by quantum simulation calculations carried out within the same study.[99]

The assignments of the molecular beam studies were in disagreement with various investigations carried out in cryogenic matrices.[91,92,100,101] Nelander[102] drew attention to this conflict and proposed that the bands at 3532 and 3545 cm^{-1} could be due to the water trimer and that instead the strong band at 3600 cm^{-1} should be attributed to the bonded OH stretch of the dimer. The recent high-resolution study of Huang and Miller[103] yielded very detailed information on the asymmetric stretch of the proton-acceptor molecule in the water dimer but was not able to resolve the conflict concerning the band position of the bonded OH stretch and locate the absorption bands of the larger water polymers.

To provide an unambiguous assignment of the absorption band near 3532 cm^{-1} to the size of the water complex (dimer or trimer) and to obtain size-specific information on the spectroscopy of the larger water polymers, we have combined molecular beam depletion spectroscopy with the kinematic cluster selection technique.[29] In a first set of experiments, carried out in Apparatus II, we have studied size-selected $(H_2O)_n$ clusters with $n = 2-5$. Later studies, carried out in Apparatus I, were devoted to the larger water clusters with $n = 7-10$ which adopt three-dimensional structures.

Finally, additional experiments were performed in Apparatus II to investigate the spectral shifts occurring when the water polymers were attached to or embedded in large rare-gas clusters. Employing the pickup technique of Scoles and co-workers,[75] we have produced and spectroscopically investigated small water complexes adsorbed on argon[73] and embedded in liquid helium[74] host clusters. Such composite clusters may be considered as mesoscopic systems

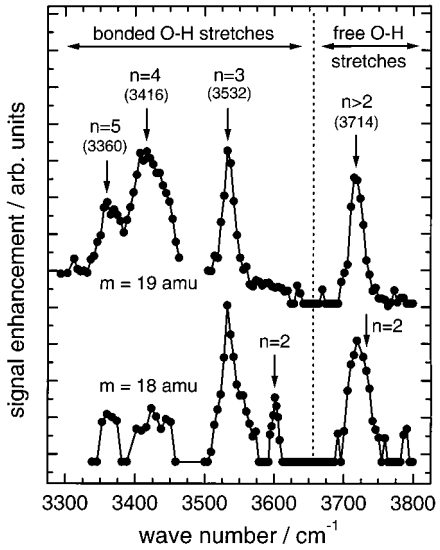

Figure 4. Absorption spectra of small water clusters ($n = 2-5$) in the OH stretch region.[73] To record these spectra, the laser-induced dissociation products were measured with the detector positioned to a small deflection angle and the mass spectrometer tuned to $m = 19$ u (upper spectrum) and $m = 18$ u (lower spectrum), respectively. In the upper spectrum, the maximum band positions in wavenumbers are given in parentheses. Their assignments to cluster sizes have been made by employing the secondary helium beam and measuring the laser-induced depletion as a function of the scattering angle (see Figure 5).

between free gas-phase polymers and molecular complexes trapped in macroscopic cryogenic rare-gas matrices and therefore deserve special attention. It will be shown that the whole set of data can be regarded as highly consistent if the frequency shifts are analyzed in terms of a correlation with the square root of the critical temperature of the gas constituting the matrix or host cluster.[104]

We note that the IR spectrum of the OH stretch mode of liquid water shows an unstructured distribution peaked at 3450 cm^{-1}. The corresponding spectrum of hexagonal ice I_h exhibits a further red-shifted peak at 3220 cm^{-1} with two shoulders at 3100 and 3380 cm^{-1}. The general shift is an indication of the stronger hydrogen bonds in the tetrahedral arrangement of the solid, while the relatively broad distribution can be traced back to the proton disorder.[105]

B. Free Clusters

1. Sizes $n = 2-5$

The first size-selective studies on free water clusters[73] were carried out in Apparatus II in the configurations shown in Figures 1b and 2b. Absorption spectra were recorded by detecting the laser-induced dissociation products at small deflection angles with the mass spectrometer tuned to $m = 18$ $[H_2O^+]$ and 19 u $[(H_2O)H^+]$. The results are summarized in Figure 4. The upper spectrum was measured at mass $m = 19$ u and $\Theta = 2.5°$, while the lower spectrum was recorded at $m = 18$ u and $\Theta = 3.5°$. Since the fragment spectrum measured on mass $m = 19$ u cannot contain contributions from dissociating water dimers (which must be monomers), the spectral features of the water dimer can be readily assigned

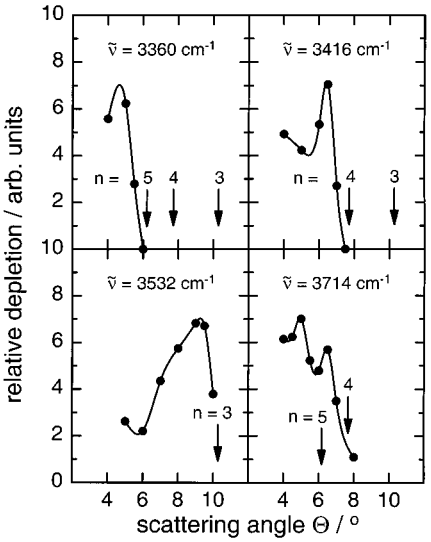

Figure 5. Relative depletion of water clusters measured as a function of the scattering angle with the secondary helium beam turned on.[73] For each curve the laser frequency $\tilde{\nu}$ was kept fixed at the maximum of an absorption band labeled in the upper spectrum of Figure 4. The positions marked by arrows indicate the maximum scattering angles as expected for the various cluster sizes n from the Newton diagram.

by comparing the two spectra. They are indicated in the $m = 18$ u spectrum by arrows labeled with $n = 2$. Note that the dimer band at 3601 cm^{-1} is rather pronounced.

The other assignments, given in the upper spectrum, are much less obvious. They were determined in a scattering experiment employing the secondary helium beam (see Figure 1b). As described in section II, the laser frequency was tuned to the maxima of the absorption bands marked by arrows in the upper spectrum of Figure 4 while the laser-induced depletion was measured as a function of the scattering angle. From the cutoff angle, the size of the cluster responsible for the absorption could be determined. The results are depicted in Figure 5. In each plot the arrows indicate the maximum deflection angles of the water clusters of size n, as calculated from the Newton diagram.[48] The first angular depletion curve, measured at $\tilde{\nu} = 3360$ cm^{-1}, goes to zero just before the maximum deflection angle of the water pentamer ($n = 5$) is reached, indicating that the corresponding absorption band must be assigned to the pentamer. In contrast, the depletion signals measured at $\tilde{\nu} = 3416$ and 3532 cm^{-1} can be observed up to the maximum tetramer and trimer deflection angles from which we conclude that tetramers and trimers are responsible for the respective absorption bands. The angular depletion curve measured for $\tilde{\nu} = 3714$ cm^{-1} shows two maxima and a cutoff below the tetramer angle. Thus, it appears that both tetramers and pentamers are contributing to the band at $\tilde{\nu} = 3714$ cm^{-1}. The latter frequency position is marked in Figure 4 by the arrow labeled with $n > 2$. All band positions and assignments discussed so far are collected in Table 1.

In agreement with earlier studies,[97,98] the present investigation has shown that the ionization-induced fragmentation of water clusters constitutes a serious problem when the spectra measured with a mass spectrometer are to be assigned to specific cluster sizes. However, with the help of the kinematic size selection (using the secondary helium beam to disperse the water complexes), it was possible to achieve a consistent interpretation. While in earlier molecular beam studies[98,99] the vibrational band near 3532 cm^{-1} was attributed to the bonded OH stretch of the water dimer, the present study clearly reveals that this assignment is wrong and that the *trimer* is responsible for this absorption band.[73] With this reassignment, the band at 3601 cm^{-1} becomes the lowest frequency dimer band and, therefore, has to be attributed to the bonded OH stretch. On the other hand, it turns out that the symmetric stretch (ν_1) of the proton-acceptor molecule, falsely located at 3601 cm^{-1},[98,99] has not yet been observed. However, this is not surprising since the ν_1 acceptor band should be at least 6 times weaker than the bonded OH band, as line-strength calculations have revealed.[106−110] This example demonstrates that the size selection is very important to obtain proper assignments of the spectral features to cluster sizes. It should be noted that the new assignment is in agreement with the results of matrix isolation studies.[102]

Up to now we have not yet discussed the vibrational modes responsible for the various absorption bands. As is quite well established by theoretical calculations,[82−84] the smaller water complexes (from trimer to pentamer) have cyclic structures. Their vibrational stretching modes are identified as either bonded OH stretches or free OH stretches, each of which has n components for a complex containing n water molecules. While these n components may be very close in frequency so that they cannot be resolved in the experiment, the separation between the free and bonded OH stretches is quite large (>130 cm^{-1}), with the bonded OH vibrations having significantly lower frequencies. Finally, the positions of the bonded OH stretching bands are shown to depend much more sensitively on the cluster size than the frequencies of the free stretching vibrations which lie close together. With these theoretical results in mind, it is quite obvious that the measured absorption bands shown in Figure 4 must be assigned, for $\tilde{\nu} < 3650$ cm^{-1}, to bonded OH stretches and, in the unresolved peak at 3720 cm^{-1}, to the free OH stretches of various water cluster sizes.

Table 1. Intramolecular Stretching Frequencies (in cm^{-1}) of Small Water Complexes in the Gas Phase and in Rare-Gas Host Clusters

size	vibration	free $(H_2O)_n$	$(H_2O)_n \cdot He_N$	$(H_2O)_n \cdot Ar_N$
$n = 2$	ν_3	3745.48[a]	3745	
	ν_1	3660 ± 5[b]		
	free OH	3735	3730	3714
	bonded OH	3601	3597.4	3576
$n = 3$	free OH	3726	3719	3705
	bonded OH	3533	3532	3516
$n = 4$	free OH	3714		
	bonded OH	3416	3390[c]	
$n = 5$	free OH	3714		
	bonded OH	3360	3350[c]	

[a] Reference 103. [b] estimated by extrapolation of the matrix data (see section III.C.3). [c] Miller, R. E. Private communication, 2000.

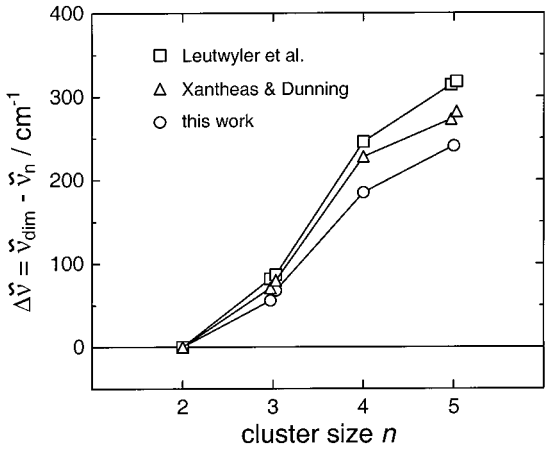

Figure 6. Comparison of the present gas-phase results on water clusters with theoretical predictions by Leutwyler et al.[82,83] and Xantheas and Dunning.[84] The frequency shifts of the bonded OH stretches of water trimer, tetramer, and pentamer rings, relative to the bonded OH stretch of the water dimer, are plotted as a function of cluster size. The experimental trimer splitting has been observed for $(H_2O)_3$ trapped in helium clusters (see section III.C.2).

Now we want to compare our gas-phase results with recent ab initio calculations. Kim et al.[111] computed water dimer frequencies at various levels of theory [HF, MP2, CCSD(T)]. Best agreement with the experimental results is obtained for a Hartree−Fock (HF) calculation with a triple-ζ plus double polarization (TZ2P) basis set, followed by the coupled-cluster calculation [CCSD(T)]. The HF/TZ2P calculation yields the following frequency shifts from the monomer ν_1 and ν_3 bands: −10 cm^{-1} for the ν_3 band of the proton acceptor, −22 cm^{-1} for the ν_3 band of the proton donor (free OH stretch), and −48 cm^{-1} for the ν_1 band of the proton donor (bonded OH stretch). Comparing these values with the respective experimental shifts (−10.5,[103] −21, and −56 cm^{-1}), the agreement must be regarded as extremely good. We note that this follows from a compensation of errors caused by the approximate basis set, the harmonic treatment, and the neglect of zero-point energy and electron correlation.

The intramolecular frequencies of the larger water polymers [$(H_2O)_n$, $n = 3-5$] were first derived by Honegger and Leutwyler[82] and Knochenmuss and Leutwyler[83] in the harmonic approximation at the SCF level. To account for the anharmonicity, the authors determined scaling factors for the monomer frequencies which were also used for the larger clusters. Since the scaled frequency of the bonded OH stretch of the dimer (3552 cm^{-1}) is significantly smaller than the experimental result (3601 cm^{-1}), it is more meaningful to compare the relative shifts from this dimer frequency rather than the absolute values. This is done in Figure 6. It is immediately seen that the qualitative behavior of the theoretical curve of Leutwyler et al.[82,83] (□) and our data (○) is the same. The theoretically predicted red shifts are consistently too large, but the overall trend is reproduced very well. If the calculated shifts are multiplied by a factor of 0.76, perfect agreement is obtained. Xantheas and Dunning[84] calculated harmonic vibrational frequencies at the MP2 level with an augmented basis set. At this higher level approach, it was not necessary to adjust the computed values. Plotting the shifts from the dimer-bonded OH stretch (ν_{dim}) as a function of cluster size, it is seen that the agreement between experiment and theory is very good, in particular if one considers that no scaling was applied. The pentamer frequencies have been calculated by Xantheas very recently.[109] Discussing vibrational frequency calculations, the new approach of Gerber and coworkers should be mentioned. These authors used the correlation-corrected vibrational self-consistent field (CC−VSCF) approximation and obtained results in fairly good agreement with the experiment. The advantage of the new approach is that anharmonicity and coupling between different vibrational modes are included.

Very recently, Paul et al.[9] studied the vibrational spectroscopy of small water clusters ($n = 2-6$) by combining the molecular beam technique with a cavity ringdown experiment. With this rather new technique, which is denoted by infrared cavity ringdown laser absorption spectroscopy (IR−CRLAS), it was possible to determine the concentration of water clusters in the beam from dimer to hexamer. The positions of the vibrational bands of the smaller water clusters ($n = 2-5$) are in close agreement with the results of the present study (see Figure 4).

Using resonant ion-dip infrared spectroscopy, Pribble and Zwier[20] studied the vibrational spectroscopy of small water clusters attached to a benzene molecule. The spectra are characterized by additional bands due to the interaction of the benzene molecule with the water complex, which breaks the degeneracy in the water ring vibrations and allows for a new hydrogen bond involving the π electron cloud of the benzene molecule. Similar experiments were carried out in Mikami's group where the water clusters were attached to a phenol molecule.[22] Here the phenol OH group takes the role of a water molecule, so that the phenol·$(H_2O)_2$ spectrum must be compared with the benzene·$(H_2O)_3$ spectrum.

2. Sizes $n = 7-10$

The experiments in the size range from $n = 7$ to 10 have been carried out for fully size-selected clusters.[113,114] The experimental arrangement is that of Apparatus I described in Figure 1a of section II.B. The clusters were prepared by an adiabatic expansion of a 15% mixture of water vapor in helium carrier gas. The detector was set to the largest possible scattering angle for each size. Clusters of larger size cannot reach this angle. To discriminate against the smaller clusters in the beam, the mass spectrometer was operated at the mass of the next smaller protonated ion, e.g., $(H_2O)_n$ was detected as $(H_2O)_{n-1}H^+$.

The results are presented in Figure 7 and Table 2. At first glance, the spectra exhibit more structure than the two groups, the free and the hydrogen-bonded OH bands which are observed in the spectra of the cyclic clusters from $n = 3$ to 5. This is clearly a reflection of their more complicated three-dimensional structure which starts with $n = 6$.[32] For the heptamer, a sort of line spectrum was measured in which each of the 14 OH groups is reflected in a

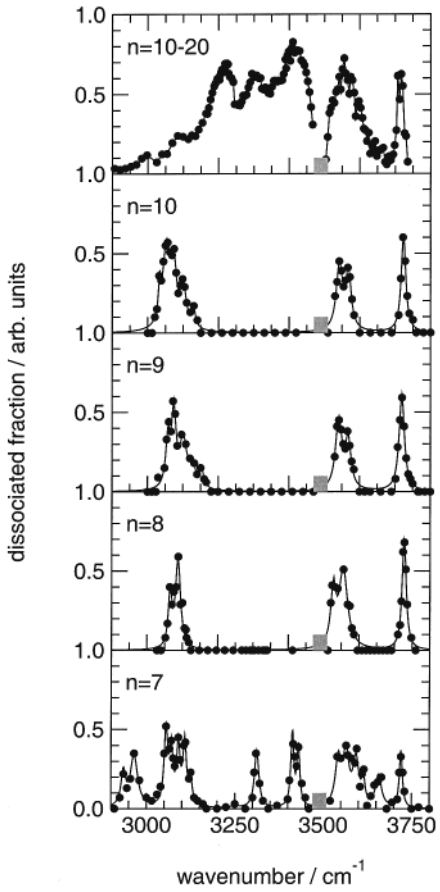

Figure 7. Measured depletion spectra of size-selected water clusters in the OH stretch region from $n = 7$ to 10.[113,114] The upper panel shows a spectrum of a cluster distribution in the size range from $n = 10$ to 20.[123] The gray block on the wavenumber axis indicates the gap of the OPO.

Table 2. Intramolecular OH Stretching Frequencies[a] of Water Clusters in the Gas Phase (in cm^{-1})[113,114]

vibration	$n = 7$	$n = 8$	$n = 9$	$n = 10$
free	3720	3727	3719	3723
IRR	3657			
DDA	3614−3543	3557	3568	3568
DDA		3528	3541	3542
IRR	3430−3413			
IRR	3312			
DA			3140	3129
DAA	3108−3055	3087[b]	3101	3100
DAA		3065[b]	3066	3063
IRR	2965[b]			
IRR	2935[b]			

[a] IRR, irregular, indicates positions which are not explained by the regular pattern of the octamer cube, the double donor DDA, and the single donor DAA. DA are 2-fold-coordinated molecules. [b] Two isomers.

different line position ranging from 3710 to 2935 cm^{-1}. This is the largest line shift ever measured for water clusters and the bulk condensed phase. For the larger clusters, the spectra are again simplified and consist essentially of three groups, now an indication of collective vibrations of the OH groups in similar environments. We note the remarkable fact that the spectra of the nonamer and decamer are, aside from some intensity around 3130 cm^{-1}, not very different from that of the octamer.

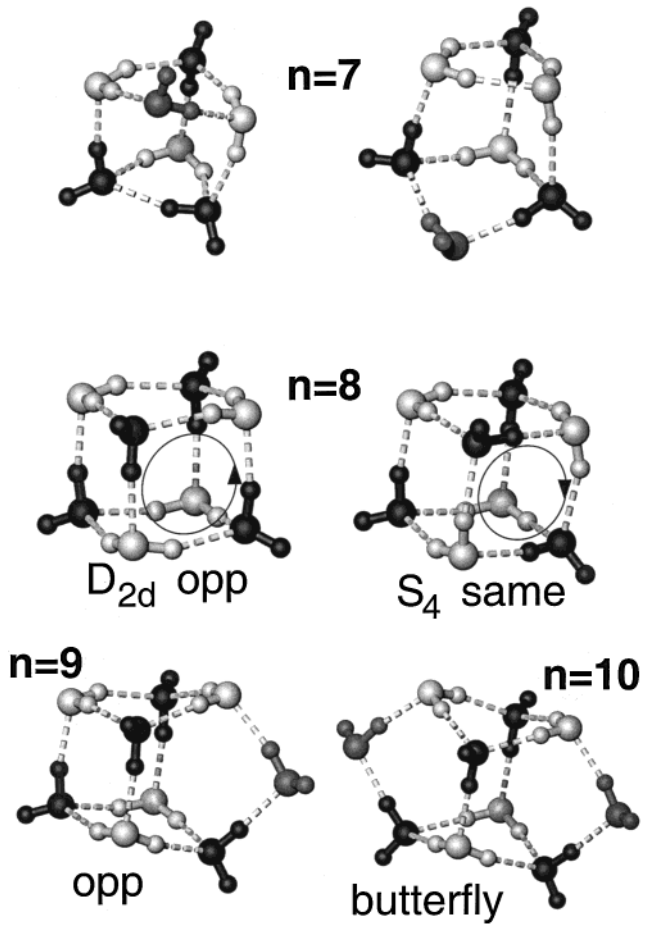

Figure 8. Calculated minimum energy configurations of water clusters from heptamer to decamer. For the heptamer and octamer, the second lowest energy isomers are presented also.[115] The DDA molecules are black, the DAA molecules white, and the DA molecules gray. Note that the two heptamers are generated by removing a DDA molecule from the upper front corner or a DAA molecule from the lower front corner of the S_4 octamer. The orientation of the hydrogen bonds in the two tetramer cycles of the octamer occur in the opposite (D_{2d}) or the same (S_4) direction.

In a very detailed effort, the experimental spectra could be completely explained by combined high-level ab initio calculations and simulations based on a polarizable model potential using permanent charges and induced dipoles.[115] In the latter case, the frequencies were calculated in a Morse oscillator basis with the help of a parametrized function of the electric field component parallel to the OH bond. The zero-point motion was explicitly taken into account. First, the contribution to the binding energies was calculated using the rigid body diffusion Monte Carlo method. Later, the force constant was averaged over the intermolecular motion also.

The structures which reproduce the measured spectra and which correspond with one exception to the minimum energy configurations are shown in Figure 8. They can be considered as members of a series, derived from the octamer cube by either insertion or removal of water molecules. The structural units of the octamer are 3-fold-coordinated molecules acting as double donor and single acceptor (DDA) (black) or as single donor and double acceptor (DAA) (white). All DDA molecules are connected only

to DAA molecules and vice versa. As already noted in the past, the cube is not perfect and the O···O distances emanating from bonds between DDA and DAA molecules tend to be longer (2.8 Å) than bonds emanating from DAA to DDA (2.6 Å) and thus the OH frequencies tend to be larger, since the hydrogen bond is weaker.[83,116,20,117,118] The reason is that the DAA bonds manage to optimize the single, linear hydrogen-bond geometry much better than the DDA molecules which have to accommodate two bonds which are bent. As a result, the OH stretch spectrum contains two well separated bands, one at 3065 cm^{-1} which can be traced back to the DAA configuration and one at 3560 cm^{-1} which corresponds to DDA molecules. The third one close to 3720 cm^{-1} is that of the unshifted free OH stretch of the DAA molecules. The splitting of the DDA band is caused by the interaction of the symmetric and asymmetric stretch of the two adjacent OH bonds. It is with 30 cm^{-1}, much smaller than the 100 cm^{-1} of the free molecules and even smaller than the 45 cm^{-1} of the solid. The reason is the change of the sign in one of the potential coupling constants which reduces the size. The splitting of the DAA band originates from two different isomers with nearly the same minimum energy but a different orientation of the hydrogen bonds in the two four-membered rings of the octamer. The one with S_4 symmetry has the same and the one with D_{2d} symmetry the opposite orientation of the bonds (see Figure 8).

The simple spectroscopic pattern of the three clearly separated bands is also observed for the two larger clusters $n = 9$ and 10. Here, the rings are extended by adding one or two 2-fold-coordinated AD molecules (see Figure 8, grey). This leads to a new line around 3130 cm^{-1} and a broadening of the DAA band. All other molecules are more or less in the same environment as they are in the octamer so that the same spectra result. We note that for the octamer and nonamer, other isomers have distinctly larger minimum energies and are thus clearly separated from the global minimum configurations. This is not the case for the decamer. Here, the configuration shown in Figure 8, the "butterfly" structure with two DA molecules, is 2.6 kcal/mol higher in energy than the configuration with two five-membered rings. This difference is reduced to 0.08 kcal/mol when the zero-point energy is taken into account. Since in the latter configuration two DDA and two DAA molecules are found in neighboring positions, the calculation gives additional spectral features between 3200 and 3500 cm^{-1}, in clear contrast to the experimental result. Obviously, this configuration can be ruled out and the potential model is still not optimal.

The spectrum of the heptamer looks completely different. There are two energetically close-lying minima corresponding to a fused three- and four-membered ring which is obtained from the S_4 octamer by removing a DDA or a DAA molecule, respectively. The two lines with the largest shifts around 2950 cm^{-1} result from DAA molecules which connect the two rings in each isomer. Aside from bands in the usual DAA (3065 cm^{-1}) and DDA (3560 cm^{-1}) frequency range, additional lines appear in the gap between 3300 and 3400 cm^{-1} which result from AD molecules and DAA or DDA molecules with adjacent molecules of the same type. It is noted that the excellent agreement of the theoretical predictions with the experimental results is only achieved by averaging over the zero-point motion.[115]

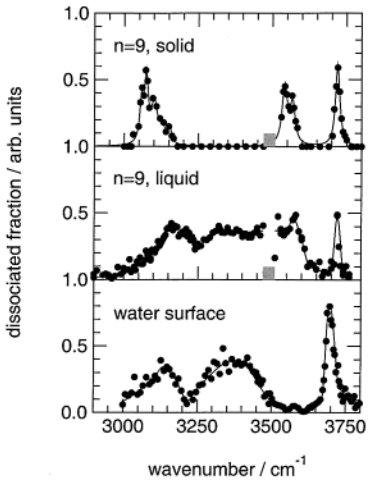

Figure 9. Measured depletion spectrum of the size-selected "liquid-like" water nonamer in the OH stretch region[130] (middle panel). For comparison, the upper panel shows the spectrum of the "solid-like" nonamer from Figure 7 and the lower panel the spectrum of the surface of bulk water.[119] The gray block on the wavenumber axis indicates the gap of the OPO.

The frequency of the free OH stretch mode is always found in the range of 3720 cm^{-1}. This is in contrast to that at 3695 cm^{-1} observed for the free OH mode for ice or water surfaces[117,119] (see also Figure 9). The reason is 2-fold. For clusters, the reduced directionality of the hydrogen bond and the lower coordination of the neighbor molecules leads to the red shift. In bulk water, the next neighbors of the surface molecules are 4-fold-coordinated, while in the small clusters we find many 3-fold-coordinated molecules which are absent in crystalline and liquid water.[120]

Data from other sources for neat, size-selected water clusters are not avaliable. There are, however, two experiments in which water clusters in this size range with the attached chromophore molecules benzene and phenol are used to probe the structure of the water clusters. In the resonant ion-dip infrared spectroscopy studies of Zwier and co-workers[20,21,28,121] the spectra of benzene$-(H_2O)_8$ are attributed to the two isomers of the cube with an attached benzene ring. Although the coupling of the benzene molecule to the water clusters is considered to be weak, there are small but distinct differences compared to the spectra shown here for neat clusters. The DAA band is split by the direct interaction with the benzene molecule so that about the same patterns results for both isomers. In the DDA band, the splitting of one of the lines is observed experimentally, since the internal temperature and thus the line width is smaller than in the experiments with the pure clusters. The conclusion that both isomers are observed comes, aside from this small difference in one of the DDA bands, from the isomer-sensitive detection and not from the different position of the single

DAA band as is observed in the case of the pure water clusters. For benzene−$(H_2O)_7$, the largest shifts of the DAA band below 3000 cm^{-1} are not observed.

Kleinermanns and co-workers measured the two-color resonant two-photon ionization spectra of phenol−$(H_2O)_n$.[24,25] The large red shift of the electronic origin by 73 cm^{-1} of phenol−$(H_2O)_8$ compared to that of phenol−H_2O is attributed to a $(H_2O)_8$ cube hydrogen bonded by one of the corner O atoms to the proton-donor phenol. For phenol−$(H_2O)_7$ they found two blue-shifted lines which they attribute to two different isomers in which the phenol is integrated as proton acceptor in one of the cycles of a cubed octamer. Thus, in this case the cubed octamer is also the preferred structural basis.

The free hexamer is a quite interesting case. It is the first size with a three-dimensional structure, and the theoretical calculations which include the zero-point motion predict the cage as the minimum energy structure to be almost degenerate with the prism.[122] The rotational constants derived from the vibration−rotation−tunneling spectrum of Saykally and co-workers[32] are in good agreement only with the cage structure. Therefore, an independent measurement of the structure using the OH stretching region would be rather interesting, since the cluster production in our experimental arrangement is quite different as might be the temperature. We plan to perform this experiment soon.

In conclusion, we note that, in the investigated size range, two different groups of clusters exist. In the "crystal-like" structures, which are observed for the cubic octamer, the nonamer, and the "butterfly" decamer, there are two well-defined groups of O···O distances based on the 3-fold-coordinated DAA and DDA molecules. In the "amorphous" type, which are observed for the heptamer and calculated for the decamer consisting of two five-membered rings, we find a distribution of different O···O distances. While the former structure leads to a few collective modes, the latter one consists of a series of lines originating from individual bonds.

Aside from these analogies in terminology, the question is often asked, whether water clusters are small models of the condensed phase. Hexagonal ice I_h consists of mainly 4-fold-coordinated water molecules in a tetrahedral arrangement of the O atoms but proton-disordered. The clusters in the size range considered here are 3-fold-coordinated and proton ordered with a different geometry, a sort of high-density version of water. Indeed, the IR spectra of ice and the clusters investigated here are totally different. If there is any analogy it comes closer to the surface of ice. However, even in this case the 3-fold-coordinated molecules of the ice surface are connected to 4-fold-coordinated ones and not, as in the clusters, to 3-fold-coordinated molecules. In addition, one-half of the molecules at the surface is still 4-fold-coordinated.[117] For larger clusters, no size-selective data are available. A measurement without size selection[123] (see Figure 7), which covers the sizes from $n = 10$ to 20, exhibits, aside from the different groups already mentioned, a peak at 3220 cm^{-1} which we attribute to 4-fold-coordinated molecules in analogy to the I_h ice spectrum. It very much resembles the results of ref 97 measured at a mass corresponding to $n = 6$ but hampered by fragmentation. The non-size-selected spectra for even larger sizes[124,9] do not show any structure and peak at 3400−3200 cm^{-1}. They are close to the spectrum of amorphous ice, a state which should be expected in a size range of 100 and more molecules.[125]

It is interesting to speculate what will happen with the clusters of the "crystalline" type if the temperature is increased. Then a large number of isomers will be available with different spectra than those of the minimum configurations which start to fill the gap between the signatures of the DAA and DDA molecules.[113] Melting-like transitions have been predicted for clusters in this size range.[126−129] Very recently we were able to detect such a transition for $(H_2O)_9$. By varying the source conditions for the cluster production (higher concentration of water vapor in the helium mixture and lower total pressure), the spectrum shown in Figure 9 resulted.[130] The pronounced peak structure of the solidlike nonamer, which is also shown in the figure, nearly disappears and is replaced by a broad distribution. For comparison, we have also plotted a recent measurement of the spectrum of the surface of water in the liquid state.[119] The similarities are quite remarkable. The two broad peaks at 3150 and 3400 cm^{-1} and the single peak at 3710 cm^{-1} are the same. They are attributed to two different types of hydrogen bonding at the liquid surface and the free OH stretch, respectively. The only difference is the DDA peak at 3550 cm^{-1}, which is not present in the bulk liquid. Apparently the "liquid-like" water nonamer resembles the bulk liquid much more than the "solid-like" nonamer, the ice I_h. The preliminary analysis of the temperature gives ca. 70 K for the measurement of the "solid-like" and 140 K for the "liquid-like" nonamer. Thus, the melting point is considerably reduced in small clusters compared to bulk water. These preliminary results have to be confirmed by calculations and a more precise determination of the temperatures by simulating the expansions. Work in this direction is in progress.

3. Conclusions

The intramolecular OH stretching vibrations of small water clusters $(H_2O)_n$ from $n = 2$ to 10 have been investigated in molecular beams using infrared depletion and fragment spectroscopy. Size-specific information was obtained by dispersing the water clusters by a helium beam. For the water dimer, three of the four predicted bands were identified. The hydrogen-bonded OH stretch is located at 3601 cm^{-1}. In agreement with all theoretical predictions, the larger clusters from $n = 3$ to 5 are cyclic with the structural unit of single proton donor and single acceptor molecules (DA). They exhibit two bands which correspond to the free and the bonded OH stretch in the ring. While the former ones fall close together near 3715 cm^{-1}, the latter ones are clearly separated and shift with increasing ring size to smaller values. The larger clusters from $n = 7$ to 10 have three-dimensional cage structures which come

in two different versions. The clusters $n = 8$ to 10 show well-ordered spectra consisting of three groups, originating from the free, the double-donor DDA, and the single-donor DAA bonds which reflect their environment. In contrast, the spectrum of the heptamer exhibits seven bands which are spread over the range from 3720 to 2935 cm^{-1}. The underlying structures for $n = 7$, 9, and 10 can be derived from the octamer cube by the removal or addition of one or two water molecules.

C. Adsorbed and Embedded Clusters

1. Argon as Host Cluster

To provide a link between the free gas-phase data just discussed and the large body of data available for water complexes trapped in macroscopic rare-gas matrices, we have investigated the vibrational spectroscopy of water molecules attached to large argon clusters.[73] Under the conditions employed in this experiment, the mean size of the argon clusters (before deposition of the water molecules) is estimated to be around $\langle N \rangle = 50$. Depletion spectra have been measured in the configuration of Figure 3a for stagnation pressures of 30 and 50 mbar in the effusive water source and with the mass spectrometer tuned to $m = 19$ [$(H_2O)H^+$] and 54 u [$(H_2O)_3^+$], respectively.

The depletion spectrum obtained for $m = 19$ u at 30 mbar stagnation pressure is dominated by three prominent absorption bands located at 3516, 3576, and 3714 cm^{-1} and closely resembles the fragment spectrum measured for free water clusters on $m =$ 18 u shown in Figure 4, except that the bands are somewhat shifted to the red.[73] On the basis of this comparison, the 3576 cm^{-1} band is readily assigned to the bonded OH stretch of the water dimer while the 3714 cm^{-1} band is due to the excitation of the free OH group in the same complex. The band at 3516 cm^{-1} is attributed to the trimer. The latter assignment becomes clear when the water pressure is raised to 50 mbar and the mass spectrometer tuned to $m = 54$ u [$(H_2O)_3^+$]. Then the 3516 cm^{-1} peak, which is assigned to the bonded OH stretch in the trimer ring, is 6 times larger. Another peak, appearing in this spectrum at 3705 cm^{-1}, is somewhat red shifted with respect to the dimer band. It is attributed to the free OH stretch of the trimer. All line positions are included in Table 1.

As can be seen from the presence of the trimer peak at 3516 cm^{-1} in the spectrum measured on $m = 19$ u [$(H_2O)H^+$], the evaporation of a monomer unit following the ionization-induced protonation reaction is an important fragmentation channel even if the water trimer is bound to the argon host cluster.[73] This indicates that the $(H_2O)_n \cdot Ar_N$ spectra measured on a specific cluster mass can be affected by the fragmentation of larger clusters and that care must be taken to interpret the data correctly. In this respect, the spectra of size-selected free water clusters are essential for a proper assignment of the observed features. On the other hand, we would like to mention that unprotonated water clusters, such as $(H_2O)_3^+$, are hardly observed if neat water clusters are ionized by electrons. It appears that the argon cluster provides an energy sink so that the usual protonation reaction is significantly quenched.[104]

It is interesting to compare the $(H_2O)_n \cdot Ar_N$ results with the band positions observed in macroscopic argon matrices.[91,92] In these studies, the band centers were determined for the bonded OH stretch of the trimer at 3516 cm^{-1}, for the bonded OH stretch of the dimer at 3574 cm^{-1}, for the trimer free OH stretch at 3700 cm^{-1}, and for the dimer free OH stretch at 3709 cm^{-1}. Comparing these values with the findings of the present study, we state that the absorption frequencies of water dimers and trimers attached to argon host clusters are very close to the values observed in conventional cryogenic argon matrices. A closer look reveals that they are slightly but consistently shifted to the gas-phase data, in particular for the free OH stretches. This indicates that the effective number of argon atoms interacting with the chromophore is smaller than in the bulk matrix. Regarding the question of whether the water complex adopts a surface or matrix site, we are tempted to conclude that the water complexes are "solvated" near the surface. The studies of Scoles and co-workers[75] have shown that the pickup technique predominantly produces surface-bound molecules. On the other hand, the close agreement with the matrix data suggests that the water complexes interact with an almost complete solvation shell. The nice agreement between the argon cluster and bulk matrix data and the close resemblance of the spectra measured for solvated and free water complexes strongly support the assignments established earlier on the basis of the size-selective experiments.

2. Helium as Host Cluster

Recent experiments have shown that helium host clusters may be considered as ideal nanomatrices with minimum interaction between the chromophore and the environment.[131] Among all possible clusters, helium clusters are the only ones which are definitely liquid. They are characterized by a very low temperature of 0.38 K, a value which was first theoretically determined[132] and later experimentally confirmed.[133] Larger helium clusters with $N > 64$ are predicted to be superfluid.[134,135] Because of these extraordinary properties, it seemed extremely interesting to study the spectroscopy of water complexes dissolved in this novel medium.

The water molecules have been embedded into the helium clusters using the pickup technique in the configuration of Figure 3b. At first, we studied the spectroscopy of the water *monomer* trapped in helium nanodroplets.[74] The studies focused on the strongest IR-active mode, the ν_3 asymmetric stretch vibration. The depletion spectrum measured with the mass spectrometer tuned to mass $m = 18$ u (H_2O^+) is characterized by three distinct absorption lines at 3730, 3778, and 3799 cm^{-1} and two weaker overlapping lines around 3760 cm^{-1}. By comparison with the free gas-phase data of water,[90,136] the stronger absorption lines can be readily attributed to the $P(1)$ (3730 cm^{-1}), $R(0)$ (3778 cm^{-1}), and $R(1)$ (3799 cm^{-1}) transitions that start from the lowest levels of *para*

[$R(0)$] and *ortho* water [$P(1)$ and $R(1)$]. Compared to the free gas phase, the lines are red shifted by 1.5−2.5 cm^{-1}. The two weaker lines are assigned to fragmented water dimers which also absorb in this frequency region (see below).

With our highest laser resolution, $\Delta\tilde{\nu} = 0.25$ cm^{-1}, we studied the strongest monomer line $R(0)$, which is practically free from dimer contributions, as a function of the helium cluster size.[74] Varying the nozzle temperature so as to change the mean cluster size between $\langle N \rangle = 1000$ and 3200, we always measured the same Lorentzian profile which was characterized by a maximum at $\tilde{\nu} = 3778$ cm^{-1} and a line width of $\Gamma = 1.5$ cm^{-1}. Thus, it appeared that, in the range investigated, the position and shape of the $R(0)$ line were independent of the helium cluster size.

Unfortunately, it was not possible to quantify the temperature of the helium clusters because only the ground states of the two nuclear spin modifications (*ortho* and *para* water) were populated. Compared to the free gas-phase case, the rotational lines were only slightly shifted to the red, indicating that the influence of the helium environment on the rotational energy levels of the water molecule was very weak and that the rotations were only slightly perturbed. Summarizing the water monomer results, it is stated that the helium host clusters induce only minor matrix shifts and that they may be considered as ideal nanomatrices for studying trapped species at extremely low temperature.

At higher water vapor pressures in the pickup chamber, two or even more water molecules may be captured by the helium host cluster. The solvated water molecules interact through their large dipole moment and form dimers and, in some cases, also larger complexes. Thus, with this technique it is possible to investigate the spectroscopy of small water polymers trapped in low-temperature nanomatrices. The spectra of the bonded and free OH stretches of the water dimer and trimer as well as the ν_3 band of the proton-acceptor molecule in the dimer have been measured for different helium cluster sizes and for various water concentrations in the pickup chamber.

Figure 10a shows a dimer depletion spectrum that we measured between 3700 and 3800 cm^{-1} with the mass spectrometer tuned to $m = 19$ u [$(H_2O)H^+$]. The nozzle temperature was $T_0 = 24$ K, resulting in a mean helium cluster size of $\langle N \rangle = 1000$, and the pressure in the pickup chamber was chosen to be $p_{H_2O} = 1.8 \times 10^{-5}$ mbar. These conditions were found by optimizing the depletion signal on mass $m = 19$ u in the main absorption band C at 3730 cm^{-1} and, on the other hand, minimizing the contribution from trimers on the basis of the count rate at $m = 37$ u [$(H_2O)_2H^+$]. The strongest band (C) at = 3730 cm^{-1} coincides with the position observed in the high-resolution study of Huang and Miller[103] for the free OH stretch of the donor molecule. The remaining weaker bands designated by A and N have been discussed in our earlier publication.[74] They belong to

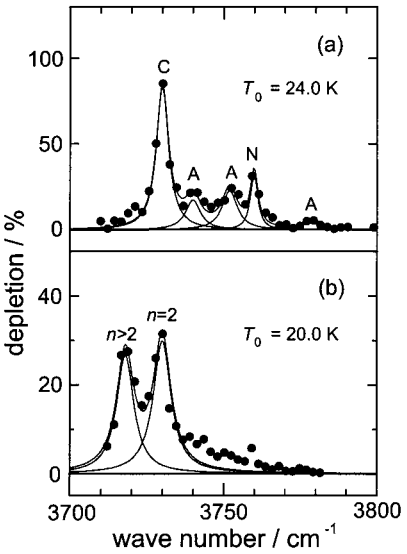

Figure 10. Variation of the absorption spectrum of small water clusters embedded in large helium droplets measured on $m = 19$ u as a function of the size of the host cluster.[74] The nozzle temperatures given in the spectra correspond to mean helium cluster sizes $\langle N \rangle = 1000$ (a) and 3200 (b) prior to the deposition of the water molecules. The pressure in the pickup chamber was 1.8×10^{-5} mbar in both experiments.

various subbands of the ν_3 proton acceptor band involving transitions between different K_a levels that have been studied under high-resolution conditions by Huang and Miller.[103] Comparison with this high-resolution study suggests that the internal-rotation-like tunneling motion is practically not hindered when the dimer is embedded in the helium cluster. This observation is in agreement with the almost free rotation found for the water monomer.

The influence of the helium cluster size on the absorption spectrum was measured on mass $m = 19$ u. If the temperature of the helium cluster source was reduced to $T_0 = 20$ K, which resulted in a helium cluster size of $\langle N \rangle = 3200$, we have measured the spectrum shown in Figure 10b. Due to the larger capturing cross section, the probability of embedding more than two water molecules is increased, and as a result, the formation of water complexes larger than the dimer is considerably enhanced. Comparing the two spectra, the most striking difference is the appearance of a strong absorption band at $\tilde{\nu} = 3719$ cm^{-1} in spectrum b. In our study on small water clusters adsorbed on Ar_N host clusters (see section III.C.1) we have found that the free OH stretch of the water trimer is red shifted by 9 cm^{-1} from the corresponding dimer absorption. Therefore, the new band at $\tilde{\nu} = 3719$ cm^{-1}, which is red shifted by 11 cm^{-1} from peak C, is assigned to the excitation of the free OH stretch in water clusters larger than the dimer (presumably trimers). From this observation we conclude again that the ionization-induced fragmentation of larger water clusters into $(H_2O)H^+$ ions ($m = 19$ u) is an important reaction channel, even if the water complexes are embedded in helium host clusters. Similar results were found for other molecules.[77] This is in contrast to an earlier study by Toennies and co-workers[137] in which it was proposed that the ionization-induced fragmentation is signifi-

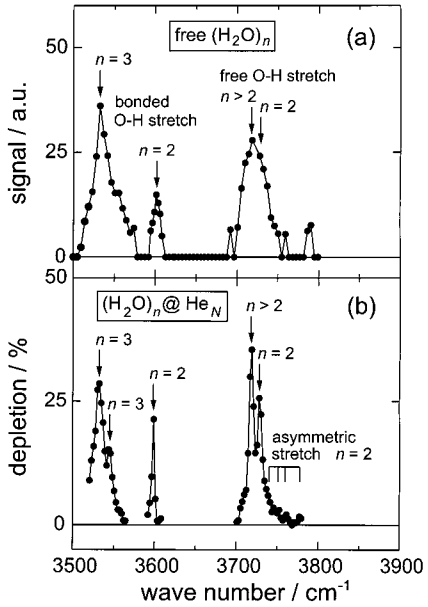

Figure 11. Comparison of spectra recorded for free water complexes (a) and water polymers embedded in large helium clusters (b).[74]

cantly reduced when the molecules are embedded in helium clusters.

As far as the bonded OH stretches of helium-embedded water polymers are concerned, the water dimer and trimer were studied. For the dimer we found a rather narrow absorption band at $\tilde{\nu} = 3598$ cm^{-1}, red shifted by 3 cm^{-1} from the gas-phase dimer absorption. A subsequent investigation of this band with higher resolution ($\Delta\tilde{\nu} = 0.25$ cm^{-1}) revealed a splitting of 1.6 cm^{-1}. The position of this doublet and the amplitude ratio of its components did not change when the host cluster size was varied from $\langle N \rangle =$ 1500 to 4200. For the trimer we found an absorption band at $\tilde{\nu} = 3532$ cm^{-1} with a satellite peak on the blue side at 3545 cm^{-1}.[74]

The essential results of the $(H_2O)_n \cdot He_N$ experiment are summarized in Figure 11, where we compare the absorption bands of free water dimers and trimers with those observed in helium host clusters. The free water cluster spectrum (a) is the same as the one shown in Figure 4. The results obtained in the helium cluster experiments are collected in the form of an overview spectrum in the lower panel (b) of Figure 11. To allow for a better comparison, we combined three measurements which were obtained under slightly different conditions. The assignments given in the figure have already been discussed.

The most striking difference between the two spectra is the fact that all spectral features are considerably narrower for $(H_2O)_n \cdot He_N$. This is due to the very low temperature encountered in the liquid helium clusters ($T = 0.38$ K).[132,133] The temperature of the free water clusters, produced in the adiabatic expansion with helium as carrier gas, is estimated to be around 80 K. Due to the reduced line widths, the free OH stretch of the dimer embedded in He_N can be clearly separated from the free OH stretch of the larger water polymers. As far as the bonded OH stretch of the water trimer is concerned, the present helium nanomatrix study clearly reveals a splitting of 13 cm. Recent ab initio calculations[88,138,139,140] as well as absorption experiments in the far-infrared[141] indicate that the water trimer has a nonplanar ring structure, giving rise to three IR-active bonded OH stretches. According to a vibrational analysis,[84] the two strongest IR bands are separated by 9 cm^{-1} whereas the third band, which is red shifted by 60 cm^{-1}, is rather weak. Although the calculated intensities of the two stronger IR-active lines are almost equal,[84] we consider the agreement between experiment and theory as rather good. Similar good agreement is obtained for the position of the free OH trimer band. Whereas theoretical predictions[84] locate the three components of this band into a small interval red shifted by 9−15 cm^{-1} from the corresponding dimer band, a red shift of 11 cm^{-1} is observed in the present study. Unfortunately, the individual components cannot be resolved with the present resolution of our OPO.

Comparing the band positions of free and helium-embedded water polymers, we obtain the following result. For water polymers trapped in helium clusters, the interaction with the environment is very weak, giving rise to rather small red shifts: 1 cm^{-1} for the trimer bonded OH stretch, 3.6 cm^{-1} for the dimer bonded OH stretch, 7 cm^{-1} for the trimer free OH stretch, 5 cm^{-1} for the dimer free OH stretch, and 1.5 cm^{-1} for the ν_3 monomer vibration [R(0) line]. As is indicated in the spectrum of Figure 11b (in the vicinity of 3750 cm^{-1}), some weak spectral features are assigned to the asymmetric stretch of the proton-acceptor molecule of the water dimer. A more detailed study of this band was presented in Figure 10.

Very recently, Nauta and Miller[142] studied the IR spectroscopy of the water hexamer embedded in helium nanodroplets. They found that the water hexamer adopted a cyclic structure and not the cage structure which is more stable in the gas phase. This interesting result was explained with the unique stepwise growth mechanism of the molecular complex and the rapid quenching provided by the helium cluster (see also section IV.C.1).

3. Conclusions

As the experiments with water polymers attached to or embedded in rare-gas clusters have shown, the fragmentation of the hydrogen-bonded complexes upon ionization still remains a severe problem although it is somewhat reduced. Therefore, the size-selective measurements on free water complexes are extremely important to interpret the spectra of solvated species correctly. When the water complexes were attached to argon host clusters, considerable red shifts were found, coming very close to the values observed in macroscopic argon matrices but without reaching them. From this observation it was concluded that the water polymers were solvated near the surface of the argon host clusters. The experiments with water polymers embedded in liquid helium clusters may be summarized as follows. Due to the extremely low temperature (0.38 K) achieved in the host cluster, the widths of the absorption bands are considerably reduced. As a result, the splitting in the bonded OH trimer band could be observed for

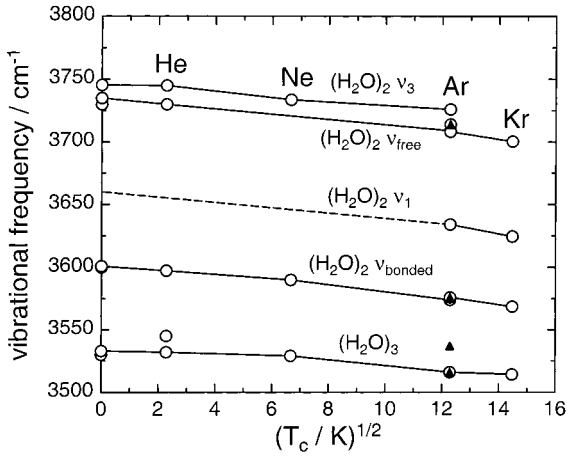

Figure 12. OH stretching frequencies of water dimers and trimers in the gas phase, embedded in helium and argon clusters and trapped in various cryogenic matrices, plotted versus $(T_c)^{1/2}$ of the corresponding matrix material.[104] The solid triangles represent the frequencies that have been measured for $(H_2O)_n \cdot Ar_N$.

the first time and the free OH stretching bands of the water dimer and trimer could be separated. In addition, it was found that the interaction between the water molecules or clusters and the helium atoms was very weak, giving rise to very small red shifts of the vibrational bands. Finally, it was found that the water monomers and dimers rotate almost freely in the helium cluster. From these observations we may conclude that the helium cluster indeed constitutes an almost ideal nanomatrix.

Comparing our results with those of the conventional matrix studies, it is useful to establish a correlation between the matrix shift and the square root of the critical temperature T_c of the matrix material as proposed by Behrens-Griesenbach et al.[143] It has been discussed in more detail in a separate paper[104] that this relationship can be easily rationalized because the strength of the attractive interaction between the chromophore and different matrix materials roughly scales with $\sqrt{T_c}$. These investigations are the first ones which locate the bonded OH stretches of water dimers and trimers in the gas phase and, in particular, the first ones devoted to the study of water polymers trapped in the novel matrix material represented by the helium cluster. Therefore, it is interesting to see how well the present data correlate with previous results obtained in macroscopic cryogenic matrices.

In Figure 12 the band positions of the OH stretching vibrations of water dimers and trimers observed in the present work and in various matrix studies[92−94] are plotted as a function of the square root of the critical temperature. It is immediately seen that for all vibrations and matrix materials considered here, the linear relationship between frequency and $\sqrt{T_c}$ is fulfilled very well. The band with the highest frequency is assigned to the asymmetric stretching vibration of the acceptor molecule in the water dimer, while the slightly lower frequency band is attributed to the free OH stretch of the donor molecule. Due to its low infrared activity, the ν_1 dimer band has not yet been observed in the only weakly interacting matrix materials neon[94] and helium[74] nor in the free gas phase.[73] This is in contrast to the anisotropic matrices D_2 and N_2, where the ν_1 band has gained enough intensity so that it can be located with sufficient accuracy.[100,144,145] Now, if the rare-gas data is extrapolated to zero such that the straight line is parallel to the line obtained for the free OH stretch, we may predict the band position of the symmetric stretch in the proton-acceptor molecule of the water dimer to be around 3660 ± 5 cm^{-1}. This value is also in very good agreement with recent ab initio calculations[110] which locate the ν_1 dimer band at 3653 cm^{-1} and predict a 18 times smaller oscillator strength for this band than for the bonded OH stretch. As already mentioned, earlier molecular beam gas-phase studies[98,99] have falsely assigned the band around 3601 cm^{-1} to the symmetric stretch. With our size-selective study, we could show that the band at 3601 cm^{-1} must be assigned to the bonded OH stretch. The correlation presented in Figure 12 nicely supports this interpretation. Furthermore, it is seen that on the basis of this correlation, a consistent picture for all four OH stretching vibrations of the water dimer is obtained.

IV. Methanol Clusters

A. Introduction

In contrast to water with its unique ability of forming tetrahedral networks, methanol can only interact by one nearly linear hydrogen bond and by hydrophobic forces around the methyl group. The crystal is built by infinite hydrogen-bonded chains of molecules with coordination number two and with adjacent chains pointing in opposite directions.[146] Similarly, the dominating structures of the liquid are chains and to a lesser extent also rings with two hydrogen bonds for every molecule. Structures with one bond per molecule (terminated chains) and three bonds per molecule (branching points) are present but with less probability as was shown by molecular dynamics simulations.[147,148] Similar results were obtained by the direct fitting of X-ray[149−151] and new neutron diffraction data.[152] In the latter case, a preference of small chains was observed in contradiction to previous results which favored cyclic hexamers.[151] It seems that the data which are currently available for the liquid phase do not provide enough details to finally decide to what extent chain and cyclic structures are present. In the gas phase, the increase in thermal conductivity as a function of pressure was attributed to the existence of cyclic tetramers.[153] Molecular beam electric deflection studies demonstrated that aside from the dimer, clusters up to $n = 17$ are strongly defocused.[154] This result is a clear indication that rings with no dipole moments are the dominating structure in this size range.

The vibrational spectra of the OH stretch mode exhibit the expected large red shifts relative to the 3681.5 cm^{-1} band of the free methanol molecule and appear at 3297 and 3193 cm^{-1} for the crystal and as a broad band which peaks at 3340 cm^{-1} for the liquid. In contrast, the CO stretch mode is 1030 and 1029 cm^{-1} for the solid and the liquid, respectively, only

marginally red shifted from the gas-phase value at 1033.5 cm^{-1}.[155] With this information available it is not surprising that size-selected methanol clusters have been thoroughly investigated by the scattering method both in the range of the OH and the CO stretch mode. In addition, there are also results available for methanol clusters interacting with helium droplets and large argon clusters. We will discuss these results separately.

B. Free Clusters

1. The OH Stretch Mode

Results for the excitation of the OH stretch mode which are based on completely size-selected beams have been available only recently. Huisken and co-workers measured the dimer[156] and the trimer[157] in Apparatus II, while Buck and co-workers took the spectra from $n = 4$ to 9[72] in Apparatus I of Figure 1. Since the OH stretch is a direct probe of the hydrogen bond, we expect a large red shift caused by the change of the interaction potential. Therefore, this system should be a critical test of any theoretical treatment both for the potential models and the method for calculating the shifts. The experimental results are shown in Figure 13 for all clusters from the dimer to the nonamer.

The dimer shows the expected two bands of the free (not shown in the figure) and the hydrogen-bonded molecules. For the trimer, three nearly equally spaced peaks are observed with the largest intensity centered at the middle peak. This is a clear indication that the trimer is not planar but slightly asymmetric. The tetramer, hexamer, and octamer show structured spectra with two or three peaks. The odd-sized clusters, the pentamer, heptamer, and nonamer, exhibit spectra with several weak humps which are, in general, broader than the corresponding next smaller even clusters. The peaks of the highest intensities shift as a function of size to smaller values from 3570 for the dimer over 3470, 3280, 3240, and 3230 cm^{-1} for $n = 3-6$ to values between 3200 and 3300 cm^{-1} for the larger clusters. These values are already close to those measured for solid methanol. Generally, the spectra of the clusters with $n \geq 4$ are much broader than those obtained for water shown in the previous section. This can have different reasons. The tetramer and pentamer are certainly influenced by the selection method in which the clusters are excited in the collision. In comparison, the line widths of the dimer and the trimer spectra which were taken for cold clusters are much smaller. For the larger clusters, this effect should gradually disappear. Therefore, either additional isomers contribute to the spectra in this size range or another intrinsic process is operating here.

Other results based on size-selected clusters are not available. Since the main bands of the smaller clusters are clearly separated from each other, we can compare our results with measurements based on cavity ringdown laser absorption spectroscopy (CRLAS)[158] or Fourier transform infrared (FTIR) spectroscopy.[159] The dimer and trimer spectra are nearly identical, and out of a broad distribution which is attributed to overlapping larger clusters, the tetramer is clearly visible. The spectra of methanol clusters with an attached benzene chromophore show similar features as those found for the neat clusters for the dimer and for $n = 4-6$,[27,28] thus indicating similar structures. For benzene$-(CH_3OH)_3$, however, a chain is found as the minimum energy configuration. Here the possible H-bonding with the π cloud of the benzene ring completely changes the minimum energy geometry.[27,28]

For the interpretation of the data we have to compare them with calculations based on the minimum energy configurations of the cluster structures. The most detailed results concerning the basis set are available for the trimer.[160,161] Larger clusters up to the hexamer have been calculated using DFT[162] and MP2 or HF methods[163,164] still with large basis sets. In all cases the frequency shifts have been obtained in the harmonic approximation. Finally, Buck et al.[165] carried out calculations with a systematic model potential which was based on monomer properties. The electrostatic part, which is the most critical one for hydrogen-bonded systems, was modeled by a distributed multipole analysis up to the quadrupole moment. The calculated structures of the clusters are shown in Figure 14. The frequency shifts were calculated in the harmonic and anharmonic approximations using both second-order perturbation theory as well as a variational approach.[165,166] The intramolecular force field is a modified version of that of ref 167. The results of these calculations are also presented in Figure 13. We chose the anharmonic approximation based on variational calculations for $n = 2$ and 3 (▼) and perturbation theory in the harmonic approximation for $n = 4$ to 9 (|).

The dimer exhibits a linear hydrogen bond, while the trimer and tetramer are nonplanar rings with C_1 and S_4 symmetry, respectively. This is in contrast to the structures calculated for the OPLS potential[168] which were planar with C_{3h} and C_{4h} symmetry, respectively. For the larger clusters, the odd ones with $n = 5$, 7, and 9 exhibit distorted rings while the even ones continue to show S_6 and S_8 symmetry. These are very symmetric structures with the methyl groups pointing alternately up and down. It is noted here that for $n = 8$ an isomeric structure close to the just mentioned minimum energy configuration also exists which is also displayed in Figure 14. It is a folded ring with S_4 symmetry.

The large red shift of the donor band in the dimer as well as the nearly unshifted line of the acceptor molecule at 3684 cm^{-1} (not shown in the figure) are reproduced by our calculation with an error of about 20 cm^{-1}. Similar results were obtained in MP2 calculations[163] and with larger deviations also in DFT calculations.[162] Recently, the dimer spectrum was measured using different techniques, namely, CRLAS[158] and FTIR spectroscopy,[159] which are not size-selective but directly proportional to the transition moment. The results agree within less than a wavenumber. In the case of the methanol dimer−benzene complex, two lines appear also. They are attributed to the excitation of the hydrogen-bonded donor and

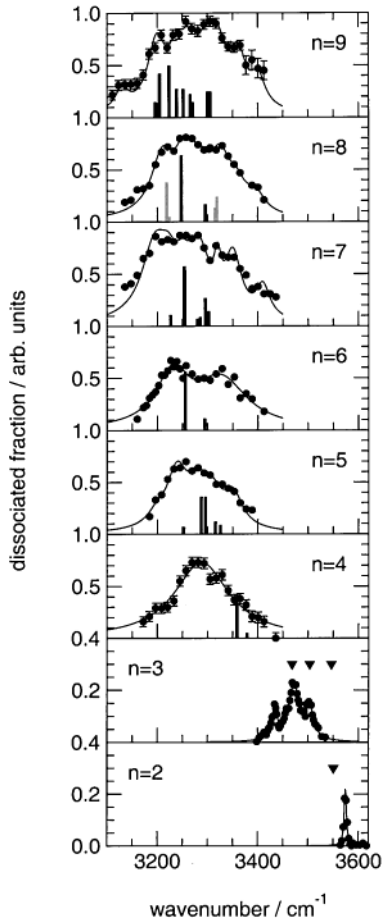

Figure 13. Measured depletion spectra of size-selected methanol clusters in the OH stretch region.[62,72,156] The sticks represent calculated bands with relative intensities using the minimum energy configurations based on the systematic potential of Wheatley[165] (see Figure 14 and the cluster approach in the harmonic approximation (n = 4−8)). For the octamer, the lines of the second lowest energy configuration also are presented by gray sticks. For n = 2 and 3, the calculated positions in the variational approach[165,166] are shown by triangles.

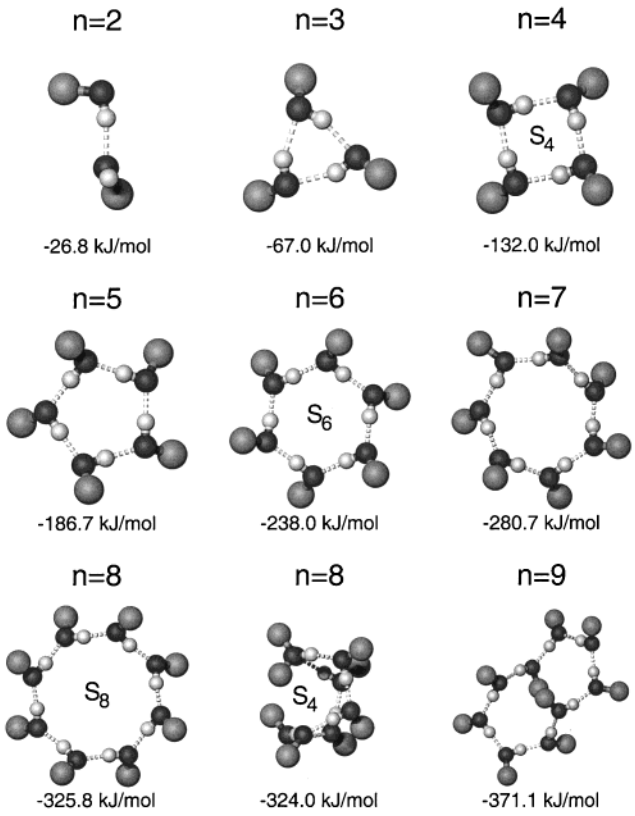

Figure 14. Calculated minimum energy configurations of methanol clusters using the systematic potential of Wheatley from dimer to nonamer.[165] For n = 8, the two lowest energy isomers are shown. The numbers denote the energies of the minimum. The CH_3 group is marked by a gray ball.

the acceptor molecule which is engaged in a hydrogen bond with the benzene π electrons.[27]

A very interesting case is the trimer. The experimental result is again completely reproduced for the line positions by the recent direct absorption experiments.[158,159] Because of the higher resolution in the latter experiments, the main band and one of the satellite bands show an additional splitting of a couple of wavenumbers. As for the intensities, there are some discrepancies which may be traced back to the different detection methods, direct absorption and predissociation. Nearly all calculations, those with very large basis sets included,[160,161] predict on the basis of the minimum configuration a nearly degenerate doublet separated by 10 wavenumbers and, with much less intensity, a third line shifted by about 60 wavenumbers to smaller values. This is the result that one would expect for a nearly planar ring with a slight asymmetry caused by the two carbon atoms of the methyl groups, one placed above and one placed below the ring. This causes the splitting of the degenerate IR-active line and gives the IR-inactive line some intensity. This result, however, is based on the harmonic oscillator analysis. Even if anharmonic corrections of each main frequency are introduced, the picture does not change. In the variational calculation, however, the quartic anharmonic couplings between the two closely lying frequencies of the type of a Darling−Dennison resonance $\langle v_1 = 2, v_2 = 0|\phi_{1122}|v_1 = 0, v_2 = 2\rangle$ are included and lead to the correct splitting of about 30 to 40 cm^{-1} between the lines.[165] The absolute shift is still off by −35 cm^{-1}, probably due to an error in the potential model. The additional splitting of two of the lines has been recently explained by invoking two further isomers, a symmetric one and the chain.[161] This explanation seems to be quite unlikely, since the correct pattern could not be reproduced. In addition, structural isomers are found in matrix studies[169,170] and helium droplets[77] (see also next section) but are less likely to occur in supersonic jet expansions. This is confirmed by the invariance of the relative intensities to different expansion conditions. A more probable explanation are combination bands with low-frequency intermolecular modes.[159] While the benzene−methanol trimer contains a chainlike methanol trimer,[27] the spectrum of fluorobenzene complexed with $(CH_3OH)_3$ also reveals, in addition to the chain structure of the methanol trimer subunit, a cyclic arrangement with three peaks[171] as was observed in the present study for the free methanol trimer.

The measured size-selected tetramer spectrum consists of a broad peak at 3280 cm^{-1} with a shoulder at higher wavenumbers. This seems to be at variance

with the direct absorption measurements[158,159] where a small, single peak at 3290 cm^{-1} emerges out of the background of the contributions from larger clusters. If we ignore, however, the intensity of one or two points, which is clearly within the experimental accuracy, a very broad distribution results with about the same peak position at 3288 cm^{-1}. The width of the band could be attributed to the internal excitation of the clusters in the selection process. The theoretically predicted second peak is of smaller intensity and not resolved in the experiment. Very recently, a new calculation of the spectrum of the methanol tetramer at the MP2 level was carried out[172] and the authors came to the conclusion that the broad distribution could result from a second isomer at the large wavenumber side and from the excitation of the symmetric band with an unresolved tunneling splitting caused by a concerted proton transfer at the low wavenumber side. A new measurement of this band, if possible at different temperatures, should solve this problem. The symmetry-breaking effect caused by the presence of the benzene molecule is also used to interpret the line splitting in the spectrum of the tetramer−benzene complex.[27]

For the interpretation of the data of the larger clusters, the calculations based on the model potential in the harmonic approximation are used.[165] The general patterns are well reproduced. The two band structures of the hexamer with S_6 symmetry and the multiline spectra of the pentamer, heptamer, and nonamer are correctly predicted. A special case is the octamer. The lowest energy configuration of S_8 symmetry should give two lines only. The spectrum, however, is much broader and shows additional peaks. This is a clear indication that another isomer contributes to the data. The second lowest isomer of S_4 symmetry, a folded ring, which exhibits additional intensity in the outer ranges, is therefore included in the comparison. This improves the agreement with the data appreciably.

We note that the good agreement between experiment and theory is probably a compensation of two effects. While the anharmonic approximation would shift the bands by about 50 wavenumbers, the use of the model potential at the HF level and the neglected zero-point motion compensates for that. In addition, there are two deficiencies for the even-numbered clusters with S_n symmetry: The predicted line splitting is too small and for the tetramer the general shift is too small also. Interestingly, the results of scaled ab initio calculations at the HF level come to similar predictions.[163] Here the splittings are a bit better, but the shift for the tetramer is also underestimated. Better predictions are obtained by the scaled ab initio calculations using the DFT[162] and the MP2 level.[172] It is interesting to note that for the interpretation of the larger benzene−methanol complexes, cyclic methanol structures are deduced also but with a partly different arrangement of the individual methanol molecules so that they can form a cavity which accepts the benzene molecule "edge-on".[27] This result clearly shows that the final structure of these complexes is partly changed by the presence of the chromophore molecule with respect to the results of the pure clusters.

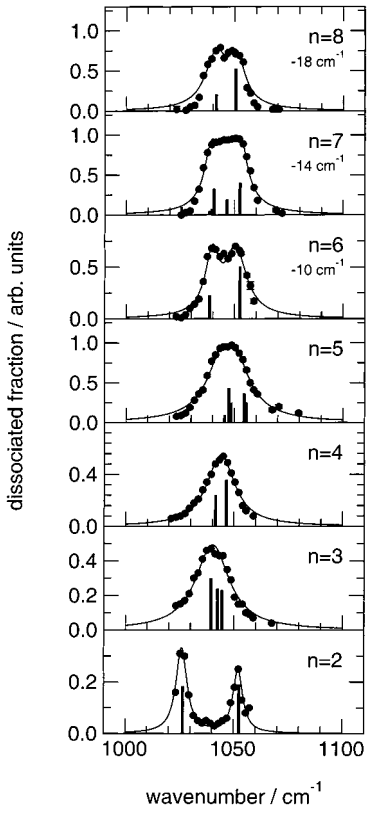

Figure 15. Measured depletion spectra of size-selected methanol clusters near the CO stretch mode of the monomer at 1033.5 cm^{-1} from refs 60, 72, and 174. The sticks represent calculated bands with relative intensities using the minimum energy configuration based on the systematic potential and the cluster approach in the anharmonic ($n = 7-8$) or the variational ($n = 2-6$) approximation.[165] The numbers in cm^{-1} indicate the shifts necessary to match the experimental results.

2. The CO Stretch Mode

In the range of the CO stretch mode near 1033.5 cm^{-1}, line-tunable CO_2 lasers were used both for cold clusters up to $n = 4$ using pulsed lasers in Apparatus II[61,62] and internally excited clusters up to $n = 6$[60,173] and, very recently, also up to $n = 8$[72] using cw lasers in Apparatus I. The experimental results agree very well with each other where they are available.[49] The spectra, shown in Figure 15, were taken in the experimental arrangement of Figure 1a except of the dimer spectrum which was measured in the configuration of Figure 2a. In the former case, the laser interacts with slightly excited complexes, while in the latter case, cold dimers are probed. Here the seeding mixture was very dilute to ensure that only dimers are in the beam.[174] This was confirmed by the good agreement with the experiments conducted with size-selected, cold species.[61,62]

The dimer spectrum is characterized by a two-peak structure with one peak shifted by -6.8 cm^{-1} to the red and another one shifted by $+18.5$ cm^{-1} to the blue compared with the frequency of the CO stretching mode of the monomer. For the next larger clusters, the trimer, tetramer, and pentamer, the experimental

data have been interpreted as resulting from one peak only, shifted to the blue by +7.5, +10.8, and +14.3 cm^{-1}, respectively. We note that the full width at half-maximum Γ is smaller for the tetramer than for the trimer and pentamer. This behavior changes with the hexamer. Now a double-peak structure appears with one peak shifted by only +6.9 cm^{-1} and the other one shifted further to the blue by +18.5 cm^{-1}. This double-peak structure is also observed for $n = 8$, while the spectrum for $n = 7$ is unstructured similar to the one for $n = 5$.

This is exactly what we would have expected from the discussion of the OH stretch mode with the big difference that the shifts are much smaller and in the other direction. We note that also for very large clusters the band is still found at 1043 cm^{-1} and does not reach the limit of the liquid or the solid at 1029 and 1030 cm^{-1}.[159]

For the dimer, the O atom of the acceptor participates directly in the bond while this is not the case for the donor. This explains the line splitting. The calculation gives a red shift for the acceptor and a larger blue shift for the donor in nearly complete agreement with the measurements. The red shift originates mainly from the elongation of the C−O distance in the attractive hydrogen bond. The blue shift results from a stronger force constant and the coupling to the OH mode which squeezes the C−O distance.

For the larger odd-sized clusters, nonplanar rings are found in the structure calculations. This behavior results in spectra in which the number of lines corresponds to the cluster size, since each CO oscillator contributes to the spectrum. This gives three lines for the trimer, five for the pentamer, and seven for the heptamer. In contrast, the even-numbered, symmetric structures with S_n symmetry exhibit two lines only. The calculations show that the two peaks originate from the coupled symmetric and antisymmetric motion of all the CO oscillators.

The predictions are in good agreement with the measurements for $n = 5-8$ as far as the form of the spectra is concerned. The hexamer and the octamer indeed exhibit a two-peak structure as predicted, while the pentamer and the heptamer show broad unstructured features caused by several lines. The absolute values of the calculations are systematically shifted to larger frequencies. This is not the case for the results of $n = 2-4$. Here the agreement is perfect with respect to the absolute scale. The large line spacings of the line-tunable laser, however, prevented us from resolving the three close-lying lines for the trimer and the two lines for the tetramer, although the lines of largest intensity match very well the measured spectra. The almost perfect agreement of calculated and measured spectra up to $n = 5$ clearly indicates the good performance of the systematic model potential in this range. The deviations which occur for the larger clusters in the absolute shift are probably caused by the potential model, which is mainly a very accurate dimer potential but neglects, aside from induction effects, repulsive three-body interactions and cooperative effects.

The explanation given in previous publications and saying that the "single" line structure of the trimer and the tetramer is an indication of a planar structure of these clusters can definitely be ruled out. The OPLS potential[168] on which these conclusions for the structures were based does not predict the correct shifts. All more realistic potential models predict for the trimer a slightly distorted planar structure which causes the degenerate IR-active band to split into two components and the symmetric IR-inactive vibration to become IR-active.

3. Conclusions

In a combined effort of size-selected measurements of the OH and CO stretch vibrations of methanol clusters from $n = 2$ to 9 and their interpretation based on a new systematic model potential, the following results were obtained. Aside from the linear chain of the dimer, all other minimum energy configurations are cyclic. The even-numbered clusters have S_n symmetry, since the methyl groups can be perfectly arranged pointing alternately up and down. This leads to simplified spectra with the collective excitation of two bands. In the experiment, they have been best resolved for the hexamer in both modes. For the tetramer, the experimental resolution was not high enough, while for the octamer another symmetric isomer starts to contribute to the signal. We note that this very symmetric S_6 hexamer structure has recently been observed by X-ray crystallography in a cavity of two hydrophobic bowl-shaped surfaces.[175] The methyl groups form only a weak contact to the hydrophobic inner surface of the cavity, so that the H-bonded hexamer can be generated. The measured O···O distance of 2.62 Å is close to the values 2.55−2.59 Å found in the calculations for the free clusters.

In the theoretical treatment of the clusters, both the systematic model potential[165] and the scaled ab initio calculation at the HF level[163] and using DFT[162] do equally well. Most of the measured patterns are correctly predicted so that the clusters can be identified. There are two interesting exceptions. The OH stretch spectrum of the trimer is only reproduced by an anharmonic variational calculation which also takes into account quartic coupling matrix elements of two close-lying frequencies. The OH stretch tetramer spectrum is quite broad, and the reasons for this behavior have still to be clarified.

The spectra in the investigated size range originate mainly from one isomer. For these clusters, which are generated in adiabatic expansions, this is usually the minimum energy configuration, a cyclic structure. For the octamer, a second cyclic isomer also contributes. Chain isomers have not been observed. In the case of the hexamer, a second isomer with four methyl groups pointing into one and the other two groups pointing into the other direction was observed after increasing the cluster temperature.[176] Calculations of the Lindemann index showed that the clusters are still solidlike in the temperature range below 200 K.[177,46] This isomer is considered to be the lowest-energy structure in the benzene−methanol hexamer complex since it can better accommodate the benzene molecule.[27]

Recent simulations of the properties of larger methanol clusters confirm these results even if the temperature is increased into the liquidlike regime.[178] In the size range between $n = 10$ and 20, bi- and polycylic structures are found, and for $n \leq 100$, they approach a spherical shape. In no case were cyclic clusters larger than the tetramer found as proposed recently in an analysis of the liquid.[151] There seems to be an interesting transition from the cyclic structures of the clusters to the chain structure of the bulk solid or liquid.

C. Adsorbed and Embedded Clusters

By the advent of the pick-up technique, it has been possible to extend the studies of free clusters to their interaction with different host clusters. Results are available both for the CO and OH stretch of small methanol clusters interacting with large helium, argon, and water clusters. Since these host clusters have completely different properties—they are a superfluid liquid, an icosahedral solid, and a hydrogen-bonded network—we will discuss the results separately.

1. Helium as Host Cluster

Large ^{4}He droplets turned out to be an ideal nanomatrix for molecular spectroscopy. The chromophore molecules migrate into the inside and exhibit the spectrum of a free rotor with modified rotational constants at a temperature of 0.38 K. The reason is the superfluidity of the helium cluster as was convincingly demonstrated in a recent experiment with OCS molecules.[179] In most of the experiments with small SF_6,[180] water,[74,40] and ammonia[181] complexes, the same structure was found as for the free clusters. Therefore, a similar behavior was expected for methanol clusters.

The measurement of the CO stretch spectrum for the dimer and the trimer, carried out in the arrangement of Figure 3b, indeed showed, aside from small shifts below 2 wavenumbers, the same results as those obtained for the free clusters.[77] To our surprise, the spectrum of the tetramer and pentamer exhibited, instead of a single bunch of narrowly lying lines around 1043 cm^{-1}, a quite broad distribution with intensity peaks around 1030 and 1050 cm^{-1}. This is demonstrated in Figure 16 for the tetramer. It contains the spectrum measured in a helium cluster of the size $\langle N \rangle = 2700$ and detected at the mass $(CH_3OH)_2H^+$ which contains contributions from the trimer and the tetramer. The large peak is attributed to the trimer. It is close to the measured free trimer absorption band shown as the dotted line. With the help of DFT calculations for a series of different isomers,[162] we found the best agreement with the spectra caused by the isomers which consist of a cyclic trimer with an attached monomer or dimer. The predicted line positions for the tetramer are presented in the upper part of Figure 16 by solid bars, while the result for the trimer is indicated as a dashed bar. When we discuss these deviations, we have to keep in mind that the cluster building process in the helium droplet, the successive capture and aggregation of the molecules at low temperature, is

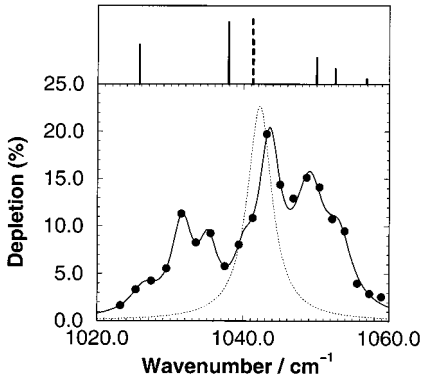

Figure 16. Measured depletion spectra of methanol trimer and tetramer embedded in large helium clusters in the region of the CO stretch mode and detected at the mass $(CH_3OH)_2H^+$.[77] The dotted line represents the measured spectrum of the free trimer. Upper panel: Calculated stick spectra of the CO stretch mode of the cyclic trimer (dotted) and the tetramer (solid) which consists of a cyclic trimer and a monomer attached to it.[77]

quite different from the cluster formation in adiabatic expansions where much more energy is available to surmount any barriers on the potential surface and to reach the global minimum. The picture which emerges from these structure determinations is as follows. The dimer and the trimer have exactly the same geometry as that observed for the free clusters, the linear hydrogen bond of an open chain for the dimer, and the cyclic arrangement for the trimer. In contrast, the tetramer and the pentamer follow a different building law, the attachment of a monomer or a dimer to the trimer ring. In spite of the low temperature of 0.38 K, the lowest energy configurations, e.g., the cyclic isomers, are not adopted. At first glance one might argue that the temperature is so low that the energy to break the trimer bond and to insert another molecule for a tetramer ring is not available. Energetic considerations based on the DFT calculation, however, show that the energy which is gained when a methanol molecule approaches the trimer is large enough for breaking the trimer bond.[77] The formation of the cyclic tetramer is obviously hindered by the fast evaporation of the helium atoms. Thus, the easiest way to generate larger clusters is the addition of a monomer and a dimer to the very stable trimer ring. Such a process should always occur when the rearrangement of the molecules takes more time than the evaporation of the helium atoms. This also explains why the building of the dimer chain and the addition to a trimer ring goes smoothly. Similar observations have been made in the OH stretch region.[182] However, the results are not as conclusive as those for the CO stretch modes, since the spectra are much broader and more difficult to disentangle. Finally, we note that a similar behavior has recently been reported for three other cases. For acetonitrile tetramers, the structure of parallel molecules is adopted in helium droplets instead of the perpendicular arrangement of the minimum energy configuration observed in the gas phase.[77] $(HCN)_n$ clusters continue to form linear chains instead of cyclic structures,[183] and water hexamers prefer to form a ring instead of the three-dimensional cage.[142] In all cases the systems do not undergo a major

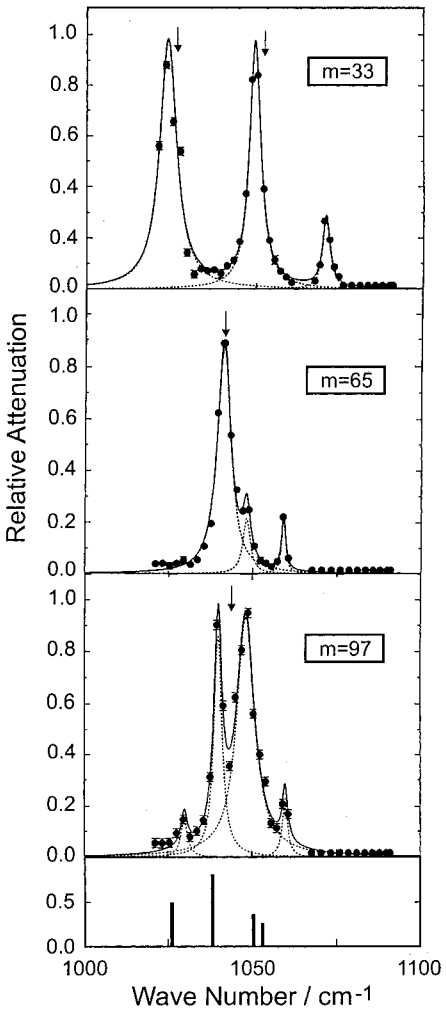

Figure 17. Measured depletion spectra of the methanol dimer, trimer, and tetramer (from top) adsorbed on large argon clusters in the region of the CO stretch and the CH_3 rock mode.[76] The arrows denote the band positions observed for the respective free methanol clusters. The stick spectrum in the bottom panel represents calculations based on a cyclic trimer with a monomer attached to it.[77]

rearrangement to reach the minimum energy configuration. Instead, they continue to add the next molecule to the already existing structure or they continue to generate, as in the case of the water hexamer, cyclic arrangements. In this way, the helium droplets are also an ideal tool for producing unusual isomers.

2. Argon as Host Cluster

Large argon clusters also provide an interesting host for spectroscopic experiments. In contrast to the helium droplets described in the last section, these clusters are usually solid and the guest molecules or small complexes are very probably adsorbed on the surface if the host cluster is large enough. The experimental results for the CO stretch excitation of small methanol complexes adsorbed on Ar_N clusters are shown in Figure 17.[76] The data taken at low pressure in the pickup source in the arrangement of Figure 3a and on the fragment mass of the dimer (m = 33 u, $(CH_3OH)H^+$) are displayed in the upper panel. They feature the well-known spectrum of the methanol dimer shifted by about 2 cm^{-1} to the red. The two large peaks are the acceptor and donor lines of the CO stretch, while the smaller peak on the blue side is attributed to the methyl rock vibration. At larger source pressures and with the mass spectrometer tuned to larger masses, the spectra of the trimer (middle panel) and tetramer (bottom panel) were obtained. In agreement with the gas-phase data,[62] the large peak of the trimer spectrum corresponds to the CO stretch and the small one to the CH_3 rock mode. Here the shift is only 1 cm^{-1}. The shoulder on the blue side of the main peak could be an indication of the small line splitting predicted theoretically for the cyclic but slightly asymmetric trimer.[165] The most interesting spectrum is that of the tetramer. Instead of the expected single band found for the gas-phase cyclic tetramer, two very distinct lines with a splitting of 8.4 cm^{-1} and an additional peak at lower frequencies of the spectrum are observed. Because of the large attenuation of almost 100%, measured in the maxima of the two major bands, it can be excluded that one of them originates from larger methanol clusters fragmenting in the ionizer. The measured pattern is exactly what has been predicted for the isomer already discussed in the last section, a cyclic trimer with a monomer attached to it. The theoretical calculations for this structure,[77] which are also presented in Figure 17, are, in view of the fact that the interaction with the argon is not accounted for, in nice agreement with the measurements. The presence of argon might also explain the deviations in the amplitudes. We can speculate about the reason for this behavior. The temperature of these doped clusters is about 30−35 K,[51,184] so that the system trapped in a local minimum does not seem to be able to overcome the barrier for breaking the trimer bond. There is, however, enough energy available for the formation of a cyclic tetramer.[77] Therefore, the more probable explanation is that the excess energy is taken away by evaporating a couple of Ar atoms so that the system stays in the given configuration which is *not* the minimum energy configuration.

3. Water as Host Cluster

Shortly after the exploration of the methanol dimer structure by measuring its CO stretching spectrum,[61] we also studied the heterodimer $CH_3OH{\cdot}H_2O$.[185] This study revealed that the methanol molecule exclusively acts as proton acceptor in this binary complex and that the other isomer, where methanol is the proton donor, is not formed in the gas phase. In contrast, the matrix studies carried out in the laboratory of Perchard[186,187] revealed different structures depending on the kind of the matrix. While the argon matrix study[187] supported our gas-phase result, it was found that in the nitrogen matrix the methanol molecule adopted the donor position.[186] In agreement with theoretical predictions,[188−193] one can conclude that the two configurations are not very different in energy and that a small perturbation may be sufficient to favor one or the other structure. Therefore, it was interesting to study the bonding of a single methanol to a large water cluster. Such a system may also be considered as a prototype of an aerosol doped with a foreign molecule, which is an interesting system in atmospheric chemistry.

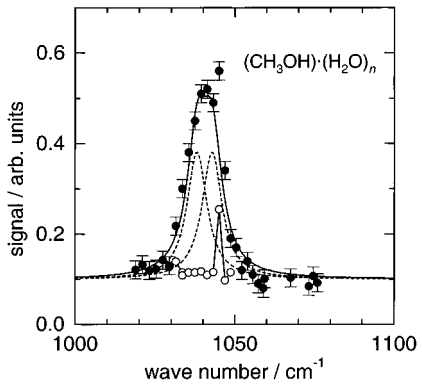

Figure 18. Dissociation spectrum of $CH_3OH\cdot(H_2O)_n$ clusters, measured on mass $m = 33$ u $[(CH_3OH)H^+]$ after exciting the CO stretch of the methanol molecule with the CO_2 laser.[123]

Employing the configuration depicted in Figure 3a, medium-sized water clusters $[(H_2O)_N, N = 15-20]$ were doped with single methanol molecules emanating from an effusive source.[123] The spectroscopy of the adsorbed methanol molecule was then studied by exciting the CO stretch with the pulsed CO_2 laser and by measuring the laser-induced depletion in the direct beam. With the mass spectrometer tuned to $m = 33$ u $[(CH_3OH)H^+]$, we have recorded the spectrum shown in Figure 18. The spectrum features a 12 cm^{-1} broad absorption band centered at 1040 cm^{-1} which is attributed to the excitation of the CO stretch in a single methanol molecule deposited on the surface of medium-sized water clusters. The data point recorded with the CO_2 laser on its 9P(22) line (1045.0 cm^{-1}) is a little bit too high. This extra intensity is due to a sharp absorption of the water host cluster at 1045 cm^{-1}, as verified by an experiment with neat water clusters[123] (see open circles). Subtracting this feature from the $CH_3OH\cdot(H_2O)_n$ spectrum, we are left with a single structureless absorption band. The attempt to fit this band with a single Lorentzian was not satisfactory. A clearly better result was obtained by taking a Gaussian function or two 7.6 cm^{-1} broad Lorentzians with their peak positions at 1038.1 and 1042.8 cm^{-1}. The sum of these two Lorentzians is represented by the solid curve.

Resorting to our previous studies on size-selected gas-phase methanol clusters[62,60] and the methanol–water binary complex,[185] we are in the position to give a rather consistent interpretation of the observed absorption band. The study on free methanol clusters has revealed that the methanol dimer CO stretching spectrum is characterized by two distinct peaks corresponding to the proton-acceptor band at 1026.5 cm^{-1} and the proton-donor band at 1051.6 cm^{-1}. This spectrum is reproduced in Figure 15. In contrast, the methanol trimer and tetramer, which are known to be cyclic, are characterized by single bands at 1042.2 and 1044.0 cm^{-1}, respectively (see Figure 15). The study of the CO stretch in the methanol–water heterodimer[185] has revealed a single band located at 1027.8 cm^{-1}, demonstrating that (i) the methanol molecule adopts the proton acceptor position in this complex and (ii) the absorption band shifts only slightly to the blue (by 1.3 cm^{-1}). The latter observation indicates that the proton-donor molecule (whether methanol or water) has only a minor effect on the CO stretching frequency of the methanol molecule acting as proton acceptor. Recent theoretical results, obtained by González et al.[192] for the methanol–water dimer and methanol$(water)_2$ trimer, are in agreement with this interpretation.

With this knowledge we conclude that the methanol molecule adsorbed on the water cluster adopts neither a simple proton-donor nor an exclusive proton-acceptor position. In contrast, it appears that the methanol molecule simultaneously plays the role of a proton donor *and* acceptor, as is the case if it is engaged in a cyclic structure. The good agreement of the higher frequency component of the absorption band, as defined by the two-Lorentzian fit, with the methanol trimer and tetramer data seems to suggest that the methanol molecule is interacting with two or three water molecules arranged in a cyclic structure. The remaining absorption on the lower frequency side is attributed to methanol molecules engaged in a third hydrogen bond between the second lone pair orbital of the oxygen and another proton-donating water molecule. According to the empirical calculations of Tarakanova,[194] this additional interaction causes a red shift of approximately 4 cm^{-1}. Thus, we obtain the result that the methanol molecule is hydrogen-bonded as proton donor and single (double) acceptor to two (or three) water molecules residing on the surface of the water cluster. This also implies that the methyl group is pointing away from the surface of the host cluster.

Our mass-spectrometric study shows that it is also possible to deposit two (or even more) methanol molecules on the water cluster. Although mass spectrometry is not able to tell whether the two methanol molecules are separated or not, we have obtained clear spectroscopic evidence that the two methanol molecules do not form a dimer, with only one methanol interacting with the water cluster. As a result, it can be assumed that if two or three methanol molecules are adsorbed by the water clusters, they reside at different positions on the surface of the host cluster. To close the discussion on the CO stretch, it should be mentioned that small $CH_3OH\cdot(H_2O)_n$ clusters were also studied by Crooks et al.[195] several years ago in a co-expansion experiment. Their spectrum, measured for the smallest cluster size, looks very similar to our result depicted in Figure 18. However, in contrast to our previous discussion, Crooks et al. interpreted their results to be consistent with the presence of just one type of hydrogen-bonded methanol molecule, acting as proton acceptor.

We have also studied the OH and CH stretching vibrations of methanol molecules attached to water clusters, using the OPO as the excitation source.[123] Since the $(H_2O)_n$ host cluster absorbs in the entire spectral region between 3000 and 3800 cm^{-1}, as is shown in Figure 7, it is difficult to detect the OH absorption band of the methanol molecule. Therefore, we have deposited the methanol molecules on deuterated water clusters which do not absorb in this spectral region. The result is a rather broad absorption spectrum containing two peaks at 3250 and 3400

cm^{-1}. This observation is in agreement with the earlier conclusion that the methanol molecule is engaged as proton donor *and* acceptor in a ring structure containing two, three, or perhaps four water molecules (besides the methanol). The study of the CH stretching vibration of methanol on D_2O clusters revealed three pronounced peaks at 2838, 2963, and 2995 cm^{-1} that could be easily assigned to the symmetric CH_3 stretch and to two components of the asymmetric CH_3 stretch, respectively. The fact that the bands are only slightly red shifted from the respective gas-phase transitions[196] (by less than 5 cm^{-1}) is in agreement with the earlier conclusion that the hydrophobic methyl group is pointing away from the host cluster.

In a final experiment, we have measured the angular distributions of the fragments, expelled from a laser-excited complex, while the CO_2 laser was tuned to the maximum of the CO stretching band.[123] We were able to detect ionic fragments as large as $CH_3OH{\cdot}(H_2O)_4H^+$ at a deflection angle of 4°. Since the neutral precursor, $CH_3OH{\cdot}(H_2O)_n$, of this ion contains at least $n = 5$ water molecules (and even more when fragmentation is taken into account), we have the result that rather large dissociation products are expelled from the doped water cluster when the methanol molecule is excited with the CO_2 laser. This observation suggests that in this experiment the water clusters did not adopt the hexagonal ice structure since the dissociation into a larger fragment, such as $CH_3OH{\cdot}(H_2O)_5$, would require the rupture of too many hydrogen bonds. Instead, the water clusters seem to be composed of loosely bound subclusters ($\langle n \rangle \approx 5$) which are easily detached from the host cluster and expelled with the chromophore into the detector.

V. Summary

The field of weakly bound neutral molecular clusters has enjoyed a remarkable growth during the last years. The main experimental tools are combinations of different spectroscopic methods with size-selecting techniques. We reported here results which are mainly based on the dispersion of the cluster sizes by the scattering from a helium beam combined with infrared photodissociation, resulting in depletion or enhancement of the beam, depending on the position of the detector. We covered the size range from $n =$ 2 to 10, but other experiments show that $n = 20$ can be reached. The tunable lasers employed are either CO_2 lasers in the 10 μm range or an OPO system around 3 μm.

The major effect of the cluster on the spectral properties of the intramolecular vibrations is to shift the spectral lines. All the systems considered here contain the OH stretch mode which is known to be a very sensitive measure of the strength of the hydrogen bonding in the system. Participating directly in the bonds, the frequencies are shifted to the red by up to 800 cm^{-1}. In the size range of $n = 6$, already the values of the condensed phase are reached and, sometimes, the cluster values even overshoot them as has been demonstrated for the water heptamer and octamer. For methanol, also the CO stretch was investigated. Here only moderate blue shifts are observed which do not converge to the nearly unshifted values of the condensed phase. In both modes, a sensitive size dependence is obtained for the clusters from $n = 2$ to 6.

All these data are strongly correlated with the structure of the clusters and the underlying interaction potential. Therefore, reliable theoretical methods were developed to first calculate the minimum energy configurations and then to determine the spectra to be compared with the experimental data. In this way, most of the measured spectral features could be explained. Although there are many ab initio calculations available in the literature, we essentially used empirical model potentials for this purpose, which were partly fit to the experimental data. In the case of methanol, the electrostatic part of the potential was modeled very carefully by means of a distributed multipole expansion. In the case of water, a polarizable model was used which was adjusted to give a balanced description of all water phases, the ferroelectric form included. Empirical potentials which are only based on fits to the liquid were not able to reproduce the data correctly.

For the calculation of the lineshifts, the usual harmonic approximation based on normal-mode analysis was not sufficient. For the methanol trimer, a variational calculation proved to be necessary to account for the correct splitting. For the water clusters, an empirical relation between the electric field and the frequency was used in a Morse potential basis. For the heptamer, agreement with the experimental data was only reached after the force constant was averaged over the intermolecular motion.

On the basis of the comparison of the experimental and calculated spectra, a clear picture of the cluster structures emerged for the investigated systems. For methanol, the chainlike structure of the dimer is related to the structure of the solid, since this is the optimum geometry for the interaction of two molecules or an arrangement of many particles which consists of subunits of chains of dimers. The clusters in the size range up to $n = 9$ behave, however, differently. They essentially form rings which are symmetric with S_n symmetry for the even-numbered clusters and a bit distorted for the odd-numbered ones, since the methyl groups cannot be arranged in an alternating up and down fashion. The reason for the ring formation is simply that the number of bonds which are now available for these structures is larger than for open chainlike arrangements. Then it does not matter that the stabilization energy per bond is usually smaller, since the ideal bonding configuration of the dimer has to be strained. The well-known cooperativity effect of the hydrogen bonds is largest for the tetramer. These rings are the dominant energetically favored isomers. For the octamer only, another cyclic, isomeric configuration is found which is nearly as stable as the global minimum.

For water clusters, the smaller ones exhibit a similar behavior. The dimer is an open linear chain, and from the trimer to the pentamer cyclic structures are found. From the hexamer onward, three-dimensional cage structures are observed. Up to the deca-

mer, they can all be derived from the cubic octamer by removing one or adding one or two molecules. Nevertheless, they appear in two different classes. The crystal-like group, which includes the cubed octamer, the lowest energy configuration of the nonamer, and the decamer, consists of essentially 3-fold-coordinated DAA and DDA molecules. They give rise to two different types of bonds and two well separated bands in the OH stretch spectrum. In contrast, the amorphous structures, which include the heptamers and the second lowest energy configuration of the decamer, are characterized by several different bonds and O···O distances which yield numerous hydrogen-bonded bands in a broad spectral range. None of these structures has any resemblance with the structure of ice or liquid water, which is dominated by 4-fold-coordinated tetrahedral arrangements where the oxygen atoms are engaged in two hydrogen and two covalent bonds.

In all cases investigated, the structures determined for the low-temperature solids are not observed for the clusters. The transition to the ordered crystalline structure of the solid usually occurs at much larger cluster sizes in the range of 100 molecules per cluster.[197,198] These values are smaller than those found for atomic van der Waals clusters but much larger than the size range considered here. It is still an open question of how the clusters behave in the size range between $n = 10$ and 20. It is expected that they consist of combinations of rings and chains with branching points and that they look like the frozen structure of a liquid or better an amorphous solid.[198] On the basis of the promising techniques introduced here, we will probably get the general answer soon.

The problem of multiple isomeric configurations has been tackled by applying double-resonance techniques which allow one to distinguish whether a line splitting is caused by nonequivalent positions in one cluster or by two different isomers.[174] In the case of the methanol hexamer, however, only the isomer with S_6 symmetry is found in the beam under expansion conditions at room temperature. By heating the nozzle and using the spectra as a fingerprint, the transition to the C_2 isomer was measured.[46,176] Such a transition has been predicted theoretically[177] and depends strongly on the potential model used. Similar results have been reported for the water nonamer. Here a liquidlike state is reached. This opens a very attractive field of new experiments, since there is not only the strong dependence on the interaction potential but also the interesting connection to the determination of size-dependent melting temperatures.

Finally, we would like to point to the new, promising field of IR spectroscopy of molecules and molecular clusters imbedded in or adsorbed on the surface of large rare-gas clusters. On the one hand, the low temperature reached especially for helium droplets simplifies the spectra like in the well-known matrix spectroscopy. On the other hand, first experiments demonstrate that due to the unique formation mechanism, it is possible to produce different isomers which are not found in the usual adiabatic expansions.

VI. Acknowledgments

U.B. acknowledges with gratitude the many contributions of his former students on both the experimental and the theoretical part, Dr. I. Ettischer, Dr. J. G. Siebers, Dr. J. Brudermann, M. Behrens, and M. Melzer as well as the input from very fruitful cooperations with Dr. R. J. Wheatley, Prof. V. Buch, and Prof. J. Sadlej on the interpretation of the data. U.B. is especially grateful to Dr. J. Brudermann for his valuable help in preparing the figures. F.H. gratefully acknowledges the contributions of his former students Dr. M. Kaloudis, Dr. M. Koch, Dr. A. Kulcke, Mr. S. Mohammad-Pooran, Dr. M. Stemmler, and Dr. O. Werhahn as well as the fruitful discussions with Dr. E. G. Tarakanova and Dr. A. A. Vigasin. Both authors would like to thank Dr. R. Fröchtenicht for his valuable help in the experiments with chromophore-embedded helium clusters. This work has been supported by the Deutsche Forschungsgemeinschaft in the Schwerpunktprogramm *Molekulare Cluster* and the Niedersachsen-Israel Programm of the Volkswagenstiftung.[1]

VII. References

(1) Scoles, G., Ed.; *The Chemical Physics of Atomic and Molecular Clusters*; North-Holland: Amsterdam, 1990.
(2) *Faraday Discuss.* **1994**, *97*, the complete issue.
(3) *Chem. Rev.* **1994**, *94*, the complete issue.
(4) *Z. Phys. D.* **1997**, *40*, the complete issue.
(5) *Chem. Phys.* **1998**, *239*, the complete issue.
(6) Nesbitt, D. J. *Chem. Rev.* **1988**, *88*, 843.
(7) Saykally, R. J. *Science* **1993**, *259*, 1570.
(8) Blake, G. A.; Laughlin, K. B.; Cohen, R. C.; Busarow, K. L.; Gwo, D.-H.; Schmuttenmaer, C. A.; Steyert, D. W.; Saykally, R. J. *Rev. Sci. Instrum.* **1991**, *62*, 1693.
(9) Paul, J. B.; Collier, C. P.; Saykally, R. J.; Scherer, J. J.; O'Keefe, A. O. *J. Phys. Chem.* **1997**, *101*, 5211.
(10) Miller, R. E. *Science* **1988**, *240*, 447.
(11) Gough, T. E.; Miller, R. E.; Scoles, G. J. *Chem. Phys.* **1978**, *69*, 1588.
(12) Miller, R. E. *J. Phys. Chem.* **1986**, *90*, 3301.
(13) Coker, D. F.; Watts, R. O. *J. Phys. Chem.* **1987**, *91*, 2513.
(14) Kappes, M.; Leutwyler, S. *Atomic and Molecular Beam Methods*; Scoles, G., Ed.; Oxford University Press: New York, 1988.
(15) Haberland, H. *Surf. Sci.* **1985**, *156*, 305.
(16) Buck, U. *J. Phys. Chem.* **1988**, *92*, 1023.
(17) Buck, U. *The Chemical Physics of Atomic and Molecular Clusters*; Scoles, G., Ed.; North-Holland: Amsterdam, 1990.
(18) Börnsen, K. O.; Lin, L. H.; Selzle, H. L.; Schlag, E. W. *J. Chem. Phys.* **1989**, *90*, 1299.
(19) Leutwyler, S. *J. Chem. Phys.* **1990**, *90*, 489.
(20) Pribble, R. N.; Zwier, T. S. *Science* **1994**, *265*, 75.
(21) Gruenloh, C. J.; Carney, J. R.; Arrington, C. A.; Zwier, T. S.; Fredericks, S. Y.; Jordan, K. D. *Science* **1997**, *276*, 1678.
(22) Watanabe, T.; Ebata, T.; Tanabe, S.; Mikami, N. *J. Chem. Phys.* **1996**, *105*, 408.
(23) Jacoby, C.; Roth, W.; Schmitt, M.; Janzen, C.; Kleinermanns, K. *J. Phys. Chem.* **1998**, *102*, 4471.
(24) Roth, W.; Schmitt, M.; Jacoby, C.; Spangenberg, D.; Janzen, C.; Kleinermanns, K. *Chem. Phys.* **1998**, *239*, 1.
(25) Janzen, C.; Spangenberg, D.; Roth, W.; Kleinermanns, K. *J. Chem. Phys.* **1999**, *110*, 9898.
(26) Barth, H. D.; Buchhold, K.; Djafari, S.; Reimann, B.; Lommatzsch, U.; Brutschy, B. *Chem. Phys.* **1998**, *239*, 49.
(27) Pribble, R. N.; Hagemeister, F.; Zwier, T. S. *J. Chem. Phys.* **1997**, *106*, 2145.
(28) Zwier, T. S. *Advances in Molecular Vibrations and Collision Dynamics*; Bowman, J., Bačić, Z., Eds.; JAI Press Inc.: Stamford, 1998.
(29) Buck, U.; Meyer, H. *Phys. Rev. Lett.* **1984**, *52*, 109.
(30) Buck, U.; Meyer, H. *J. Chem. Phys.* **1986**, *84*, 4854.
(31) Liu, K.; Cruzan, J. D.; Saykally, R. J. *Science* **1996**, *271*, 929.
(32) Liu, K.; Brown, M. G.; Carter, C.; Saykally, R. J.; Gregory, J. K.; Clary, D. C. *Nature* **1996**, *381*, 501.
(33) Liu, K.; Brown, M. G.; Saykally, R. J. *J. Phys. Chem.* **1997**, *101*, 8995.

(34) Buck, U. *Dynamics of Polyatomic van der Waals Complexes*; Halberstadt, N., Janda, K., Eds.; NATO ASI Series: New York, 1990.
(35) Buck, U. *Atomic Physics 13*; Walther, H., Hänsch, T., Neizert, B., Eds.; American Institute of Physics: New York, 1992.
(36) Buck, U. *Ber. Bunsen-Ges. Phys. Chem.* **1992**, *96*, 1275.
(37) Buck, U. *Dynamical Processes in Molecular Physics*; Delgado-Barrio, G., Ed.; IOP: Bristol, 1993.
(38) Huisken, F.; Kaloudis, M.; Kulcke, A.; Voelkel, D. *Infrared Phys. Technol.* **1995**, *36*, 171.
(39) Huisken, F.; Kaloudis, M.; Koch, M.; Kulcke, A. *Proc. SPIEE* **1997**, *3090*, 33.
(40) Tarakanova, E. G.; Huisken, F.; Kaloudis, M. *Proc. SPIEE* **1997**, *3090*, 180.
(41) Huisken, F.; Mohammad-Pooran, S.; Werhahn, O. *Recent Theoretical and Experimental Advances in Hydrogen-Bonded Clusters*; Xantheas, S. S., Ed.; Kluwer Academic Publishers: Dordrecht, 1999.
(42) Huisken, F. *Recent Theoretical and Experimental Advances in Hydrogen-Bonded Clusters*; Xantheas, S. S., Ed.; Kluwer Academic Publishers: Dordrecht, 1999.
(43) Buck, U. *J. Phys. Chem.* **1994**, *98*, 5190.
(44) Buck, U. *Clusters of Atoms and Molecules*; Haberland, H., Ed.; Springer: Berlin, 1994.
(45) Buck, U.; Ettischer, I. *Faraday Discuss. Chem. Soc.* **1994**, *97*, 215.
(46) Buck, U. *Advances in Molecular Vibrations and Collision Dynamics*; Bowman, J., Bačić, Z., Eds.; JAI Press Inc.: Stamford, 1998.
(47) Huisken, F. *Molecular Complexes in Earth's, Planetary, Cometary, and Interstellar Atmospheres*; Vigasin, A. A., Slanina, Z., Eds.; World Scientific: Singapore, 1998.
(48) Huisken, F. *Adv. Chem. Phys.* **1992**, *81*, 63.
(49) Buck, U. *Adv. At. Mol. Opt. Phys.* **1995**, *35*, 121.
(50) Huisken, F.; Pertsch, T. *Chem. Phys.* **1988**, *126*, 213.
(51) Rohmund, F.; Huisken, F. *J. Chem. Phys.* **1997**, *107*, 1045.
(52) Beu, T. A.; Buck, U.; Ettischer, I.; Hobein, M.; Siebers, J. G.; Wheatley, R. *J. Chem. Phys.* **1997**, *106*, 6806.
(53) Siebers, J. G.; Buck, U.; Beu, T. A. *Chem. Phys.* **1998**, *239*, 549.
(54) Huisken, F.; Kaloudis, M.; Kulcke, A.; Laush, C.; Lisy, J. M. *J. Chem. Phys.* **1995**, *103*, 5366.
(55) Huisken, F.; Tarakanova, E. G.; Vigasin, A. A.; Yukhnevich, G. V. *Chem. Phys. Lett.* **1995**, *245*, 319.
(56) Ehbrecht, M.; de Meijere, A.; Stemmler, M.; Huisken, F. *J. Chem. Phys.* **1992**, *97*, 3021.
(57) Ehbrecht, M.; Huisken, F. *J. Phys. Chem. A* **1997**, *101*, 7768.
(58) Baumfalk, R.; Buck, U.; Frischkorn, C.; Gandhi, S. R.; Lauenstein, C. *Ber. Bunsen-Ges. Phys. Chem.* **1997**, *101*, 606.
(59) Buck, U.; Lauenstein, C.; Rudolph, A. *Z. Phys. D* **1991**, *18*, 181.
(60) Buck, U.; Gu, X. J.; Lauenstein, C.; Rudolph, A. *J. Chem. Phys.* **1990**, *92*, 6017.
(61) Huisken, F.; Stemmler, M. *Chem. Phys. Lett.* **1988**, *144*, 391.
(62) Huisken, F.; Stemmler, M. *Z. Phys. D* **1992**, *24*, 277.
(63) LaCosse, J.; Lisy, J. M. *J. Chem. Phys.* **1991**, *94*, 4398.
(64) Klemperer, W. *Ber. Bunsen-Ges. Phys. Chem.* **1974**, *78*, 129.
(65) Ewing, G. E. *Faraday. Discuss. Chem. Soc.* **1982**, *73*, 325.
(66) Geraedts, J.; Setiadi, S.; Stolte, S.; Reuss, J. *Chem. Phys. Lett.* **1981**, *78*, 277.
(67) Fischer, G.; Miller, R. E.; Watts, R. O. *Chem. Phys.* **1983**, *80*, 147.
(68) Vernon, M. F.; Lisy, J. M.; Krajnovich, D. J.; Tramer, A.; Kwok, H. S.; Shen, Y. R.; Lee, Y. T. *Faraday Discuss. Chem. Soc.* **1982**, *73*, 387.
(69) Casassa, M. P.; Bomse, D. S.; Janda, K. C. *J. Chem. Phys.* **1981**, *74*, 5044.
(70) Hoffbauer, M. A.; Liu, K.; Giese, C. F.; Gentry, W. R. *J. Chem. Phys.* **1983**, *78*, 5567.
(71) Fraser, G. T.; Nelson, D. D.; Charo, A.; Klemperer, W. *J. Chem. Phys.* **1985**, *82*, 2435.
(72) Buck, U.; Ettischer, I. *J. Chem. Phys.* **1998**, *108*, 33.
(73) Huisken, F.; Kaloudis, M.; Kulcke, A. *J. Chem. Phys.* **1996**, *104*, 17.
(74) Fröchtenicht, R.; Kaloudis, M.; Koch, M.; Huisken, F. *J. Chem. Phys.* **1996**, *105*, 6128.
(75) Gough, T. E.; Mengel, M.; Rowntree, P. A.; Scoles, G. *J. Chem. Phys.* **1985**, *83*, 4958.
(76) Huisken, F.; Stemmler, M. *J. Chem. Phys.* **1993**, *98*, 7680.
(77) Behrens, M.; Fröchtenicht, R.; Hartmann, M.; Siebers, J. G.; Buck, U. *J. Chem. Phys.* **1999**, *111*, 2436.
(78) Huisken, F.; Kulcke, A.; Voelkel, D.; Laush, C.; Lisy, J. M. *Appl. Phys. Lett.* **1993**, *62*, 805.
(79) Huisken, F.; Pertsch, T. *Rev. Sci. Instrum.* **1987**, *58*, 1038.
(80) Dyke, T. R.; Muenter, J. S. *J. Chem. Phys.* **1972**, *57*, 5011.
(81) Del Bene, J. E.; Pople, J. A. *J. Chem. Phys.* **1970**, *52*, 4858.
(82) Honegger, E.; Leutwyler, S. *J. Chem. Phys.* **1988**, *88*, 2582.
(83) Knochenmuss, R.; Leutwyler, S. *J. Chem. Phys.* **1992**, *96*, 5233.
(84) Xantheas, S. S.; Dunning, T. H., Jr. *J. Chem. Phys.* **1993**, *99*, 8774.
(85) Gonzales, L.; Mo, O.; Yanez, M.; Elguero, J. *J. Mol. Struct.* (THEOCHEM) **1996**, *371*, 1.
(86) Kim, K.; Kim, K. S. *J. Chem. Phys.* **1998**, *109*, 5886.
(87) Kim, J.; Mujumdar, D.; Lee, H. M.; Kim, K. S. *J. Chem. Phys.* **1999**, *110*, 9128.
(88) Xantheas, S. S. *J. Chem. Phys.* **1995**, *102*, 4504.
(89) *Recent Theoretical and Experimental Advances in Hydrogen-Bonded Clusters*; Xantheas S. S., Ed.; *NATO ASI Series C*; Kluver Academic Publishers: Dordrecht: 2000.
(90) Fraley, P. E.; Rao, K. N. *J. Mol. Spectrosc.* **1969**, *29*, 348.
(91) Ayers, G. P.; Pullin, A. D. E. *Spectrochim. Acta Part A* **1976**, *32*, 1629.
(92) Bentwood, R. M.; Barnes, A. J.; Orville-Thomas, W. J. *J. Mol. Spectrosc.* **1980**, *84*, 391.
(93) Engdahl, A.; Nelander, B. *J. Mol. Struct.* **1989**, *193*, 101.
(94) Forney, D.; Jacox, M. E.; Thompson, W. E. *J. Mol. Spectrosc.* **1993**, *157*, 479.
(95) Paul, J. B.; Provencal, R. A.; Chapo, C.; Roth, K.; Casaes, R.; Saykally, R. J. *J. Phys. Chem. A* **1999**, *103*, 2972.
(96) Goss, L.; Sharpe, S. W.; Blake, T. A.; Vaida, V.; Brault, J. W. *J. Phys. Chem. A* **1999**, *103*, 103.
(97) Vernon, M. F.; Krajnovich, D. J.; Kwok, H. S.; Lisy, J. M.; Shen, Y. R.; Lee, Y. T. *J. Chem. Phys.* **1982**, *77*, 47.
(98) Page, R. H.; Frey, J. G.; Shen, Y. R.; Lee, Y. T. *Chem. Phys. Lett.* **1984**, *106*, 373.
(99) Coker, D. F.; Miller, R. E.; Watts, R. O. *J. Chem. Phys.* **1985**, *82*, 3554.
(100) Fredin, L.; Nelander, B.; Ribbegård, G. *J. Chem. Phys.* **1977**, *66*, 4065.
(101) Engdahl, A.; Nelander, B. *J. Chem. Phys.* **1987**, *86*, 1819.
(102) Nelander, B. *J. Chem. Phys.* **1988**, *88*, 5254.
(103) Huang, Z. S.; Miller, R. E. *J. Chem. Phys.* **1989**, *91*, 6613.
(104) Huisken, F.; Kaloudis, M.; Vigasin, A. A. *Chem. Phys. Lett.* **1997**, *269*, 235.
(105) Buch, V.; Devlin, J. P. *J. Chem. Phys.* **1999**, *110*, 3437.
(106) Zilles, B. A.; Person, W. B. *J. Chem. Phys.* **1983**, *79*, 65.
(107) Swanton, D. J.; Bacskay, G. B.; Hush, N. S. *Chem. Phys.* **1983**, *82*, 303.
(108) Amos, R. D. *Chem. Phys.* **1986**, *104*, 145.
(109) Xantheas, S. S. Private communication, 1997.
(110) Low, G. R.; Kjaergaard, H. G. *J. Chem. Phys.* **1999**, *110*, 9104.
(111) Kim, J.; Lee, J. Y.; Lee, S.; Mhin, B. J.; Kim, K. S. *J. Chem. Phys.* **1995**, *102*, 310.
(112) Jung, J. O.; Gerber, R. B. *J. Chem. Phys.* **1996**, *105*, 10332. Chaban, G. M.; Jung, J. O.; Gerber, R. B. *J. Phys. Chem.* **2000**, *104*, 2772.
(113) Buck, U.; Ettischer, I.; Melzer, M.; Buch, V.; Sadlej, J. *Phys. Rev. Lett.* **1998**, *80*, 2578.
(114) Brudermann, J.; Melzer, M.; Buck, U.; Kazimirski, J.; Sadlej, J.; Buch, V. *J. Chem. Phys.* **1999**, *110*, 10649.
(115) Sadlej, J.; Buch, V.; Kazimirski, J.; Buck, U. *J. Phys. Chem. A* **1999**, *103*, 4933.
(116) Jensen, J. O.; Krishnan, P. N.; Burke, L. A. *Chem. Phys. Lett.* **1995**, *246*, 13.
(117) Rowland, B.; Kadagathur, S.; Devlin, J. P.; Buch, V.; Feldmann, T.; Wojcik, M. *J. Chem. Phys.* **1995**, *102*, 8328.
(118) Kim, K.; Jordan, K. D.; Zwier, T. S. *J. Am. Chem. Soc.* **1994**, *116*, 11568.
(119) Baldelli, S.; Schnitzer, C.; Campbell, D. J.; Shultz, M. J. *J. Phys. Chem. B* **1999**, *103*, 2789.
(120) Jiang, J. C.; Chang, J. C.; Wang, B. C.; Lin, S. H.; Lee, Y. T.; Chang, H. C. *Chem. Phys. Lett.* **1998**, *289*, 373.
(121) Gruenloh, C. J.; Carney, J. R.; Hagemeister, F. C.; Arrington, C. A.; Zwier, T. *J. Chem. Phys.* **1998**, *109*, 6601.
(122) Gregory, J. K.; Clary, D. C. *Advances in Molecular Vibrations and Collision Dynamics*; Bowman, J., Bačić, Z., Eds.; JAI Press Inc.: Stamford, 1998.
(123) Huisken, F.; Mohammed-Pooran, S.; Werhahn, O. *Chem. Phys.* **1998**, *239*, 11.
(124) Page, R.; Vernon, M. F.; Shen, Y. R.; Lee, Y. T. *Chem. Phys. Lett.* **1987**, *141*, 1.
(125) Torchet, G.; Schwartz, P.; Farge, J.; de Feraudy, M. F.; Raoult, B. *J. Chem. Phys.* **1983**, *79*, 6196.
(126) Farantos, S. C.; Kapetanikis, S.; Vegiri, A. *J. Phys. Chem.* **1993**, *97*, 1993.
(127) Wales, D. J.; Ohmine, I. *J. Phys. Chem.* **1993**, *98*, 7245.
(128) Tsai, C. J.; Jordan, K. D. *J. Chem. Phys.* **1993**, *99*, 6957.
(129) Pedulla, J. M.; Jordan, K. *Chem. Phys.* **1999**, *239*, 593.
(130) Brudermann, J.; Buck, U. 1999, unpublished results.
(131) Toennies, J. P. *Helium Clusters*; Proceedings of the International School of Physics "Enrico Fermi", Course CVII; Scoles, G., Ed.; North-Holland: Amsterdam, 1990.
(132) Brink, D. M.; Stringari, S. *Z. Phys. D* **1990**, *15*, 257.
(133) Hartmann, M.; Miller, R. E.; Toennies, J. P.; Vilesov, A. *Phys. Rev. Lett.* **1995**, *75*, 1566.
(134) Krishna, M. V. R.; Whaley, K. B. *Phys. Rev. Lett.* **1990**, *64*, 1126.
(135) Sindzingre, B. P.; Klein, M. L.; Ceperley, D. M. *Phys. Rev. Lett.* **1989**, *63*, 1601.

(136) Camy-Peyret, C.; Flaud, J. M.; Guelachvili, G.; Amiot, C. *Mol. Phys.* **1973**, *26*, 825.
(137) Lewerenz, M.; Schilling, B.; Toennies, J. P. *J. Chem. Phys.* **1995**, *102*, 8191.
(138) Schütz, M.; Bürgi, T.; Leutwyler, S.; Bürgi, H. B. *J. Chem. Phys.* **1993**, *99*, 5228.
(139) van Duijneveldt-van de Rijdt, J. G. C. M.; van Duijneveldt, F. B. *Chem. Phys.* **1993**, *175*, 271.
(140) González, L.; Mó, O.; Yáñez, M.; Elguero, J. *J. Mol. Struct.* (THEOCHEM) **1996**, *371*, 1.
(141) Liu, K.; Elrod, M. J.; Loeser, J. G.; Cruzan, J. D.; Pugliano, N.; Brown, M. G.; Rzepiela, J.; Saykally, R. *J. Faraday Discuss.* **1994**, *97*, 35.
(142) Nauta, K.; Miller, R. E. *Science* **2000**, *287*, 293.
(143) Behrens-Griesenbach, A.; Luck, W. A. P.; Schrems, O. *J. Chem. Soc., Faraday Trans.* **1984**, *80*, 579.
(144) Murby, E. J.; Pullin, A. D. E. *Austr. J. Chem.* **1979**, *32*, 1167.
(145) Tursi, A. J.; Nixon, E. R. *J. Chem. Phys.* **1970**, *52*, 1521.
(146) Torrie, B. H.; Weng, S. X.; Powell, B. M. *Mol. Phys.* **1989**, *67*, 575.
(147) Jorgensen, W. I. *J. Am. Chem. Soc.* **1980**, *102* (2), 543.
(148) Palinkas, G.; Hawlicka, E.; Heinzinger, K. *J. Phys. Chem.* **1987**, *91*, 4334.
(149) Magini, M.; Paschina, G.; Piccaluga, G. *J. Chem. Phys.* **1982**, *77*, 2051.
(150) Narten, A. H.; Habenschuss, A. *J. Chem. Phys.* **1984**, *80*, 3387.
(151) Sarkar, S.; Joarder, R. N. *J. Chem. Phys.* **1993**, *99*, 2032.
(152) Yamaguchi, Y.; Hikada, K.; Soper, A. K. *Mol. Phys.* **1989**, *67*, 575.
(153) Curtiss, L. A.; Blander, M. *Chem. Rev.* **1988**, *88*, 827.
(154) Kay, B.; Castleman, A. W., Jr. *J. Phys. Chem.* **1985**, *89*, 4867.
(155) Falk, M.; Whalley, E. M. *J. Chem. Phys.* **1961**, *34*, 1554.
(156) Huisken, F.; Kulcke, A.; Laush, C.; Lisy, J. *J. Chem. Phys.* **1991**, *95*, 3924.
(157) Huisken, F.; Kaloudis, M.; Koch, M.; Werhahn, O. *J. Chem. Phys.* **1996**, *105*, 8965.
(158) Provencal, R. A.; Paul, J. B.; Roth, K.; Casaes, R. N.; Saykally, R. J.; Tschumper, G. S.; Schaefer, H. F., III *J. Chem. Phys.* **1999**, *110*, 4258.
(159) Häber, T.; Schmitt, U.; Suhm, M. *Phys. Chem. Chem. Phys.* **1999**, *1*, 5573.
(160) Mó, O.; Yáñez, M.; Elguero, J. *J. Chem. Phys.* **1997**, *107*, 3592.
(161) Tschumper, G. S.; Gonzales, J. M.; Schaefer, H. F., III *J. Chem. Phys.* **1999**, *111*, 3027.
(162) Hagemeister, F.; Gruenloh, C. J.; Zwier, T. *J. Phys. Chem. A* **1998**, *102*, 82.
(163) Sauer, J.; Bleiber, A. *Pol. J. Chem.* **1998**, *72*, 1524.
(164) Sum, A. K.; Sandler, S. I. *J. Phys. Chem. A* **2000**, *104*, 1121.
(165) Buck, U.; Siebers, J. G.; Wheatley, R. J. *J. Chem. Phys.* **1998**, *108*, 20.
(166) Buck, U.; Siebers, J. G. *Eur. Phys. J. D* **1988**, *1*, 207.
(167) Schlegel, H. B.; Wolfe, S.; Bernardi, F. *J. Chem. Phys.* **1977**, *67*, 4181.
(168) Jorgensen, W. L. *J. Phys. Chem.* **1986**, *90*, 1276.
(169) Coussan, S.; Loutellier, A.; Perchard, J. P.; Racine, S.; Peremans, A.; Tadjeddine, A.; Zheng, W. Q. *J. Chem. Phys.* **1997**, *107*, 6526.
(170) Coussan, S.; Boutellier, Y.; Loutellier, A.; Perchard, J. P.; Racine, S.; Peremans, A.; Zheng, W.; Tadjeddine, A. *Chem. Phys.* **1997**, *219*, 221.
(171) Buchhold, K.; Reimann, B.; Djafari, S.; Barth, H. D.; Brutschy, B.; Tarakeshwar, P.; Kim, K. S. *J. Chem. Phys.* **2000**, *112*, 1844.
(172) Verner, M. V.; Sauer, J. Private communication, 2000.
(173) Buck, U.; Gu, X. J.; Lauenstein, C.; Rudolph, A. *J. Phys. Chem.* **1988**, *92*, 5561.
(174) Buck, U.; Hobein, M. *Z. Phys. D* **1993**, *28*, 331.
(175) Penkert, F. N.; Weyermüller, T.; Wieghardt, K. *Chem. Commun.* **1998**, *557*.
(176) Buck, U.; Ettischer, I. *J. Chem. Phys.* **1994**, *100*, 6974.
(177) Buck, U.; Schmidt, B.; Siebers, J. G. *J. Chem. Phys.* **1993**, *99*, 9428.
(178) Wright, D.; El-Shall, M. S. *J. Chem. Phys.* **1996**, *105*, 11199.
(179) Grebenev, S.; Toennies, J. P.; Vilesov, A. F. *Science* **1998**, *279*, 2083.
(180) Hartmann, M.; Miller, R. E.; Toennies, J. P.; Vilesov, A. F. *Science* **1996**, *272*, 1631.
(181) Behrens, M.; Buck, U.; Fröchtenicht, R.; Hartmann, M.; Havenith, M. *J. Chem. Phys.* **1997**, *107*, 7179.
(182) Kaloudis, M. Infrarotspektroskopie an wasserstoffbrückengebundenen Komplexen, Ph.D. Thesis, University of Göttingen 1996.
(183) Nauta, K.; Miller, R. E. *Science* **1999**, *283*, 1895.
(184) Farges, J.; de Feraudy, M. F.; Raoult, B.; Torchet, G. *J. Chem. Phys.* **1986**, *84*, 3491.
(185) Huisken, F.; Stemmler, M. *Chem. Phys. Lett.* **1991**, *180*, 332.
(186) Bakkas, N.; Bouteiller, Y.; Loutellier, A.; Perchard, J. P.; Racine, S. *J. Chem. Phys.* **1993**, *99*, 3335.
(187) Bakkas, N.; Bouteiller, Y.; Loutellier, A.; Perchard, J. P.; Racine, S. *Chem. Phys.* Lett. **1995**, *232*, 90.
(188) Del Bene, J. E. *J. Chem. Phys.* **1971**, *55*, 4633.
(189) Tse, Y.-C.; Newton, M. D.; Allen, L. C. *Chem. Phys. Lett.* **1980**, *75*, 350.
(190) Bolis, G.; Clementi, E.; Wertz, D. H.; Scheraga, H. A.; Tosi, C. *J. Am. Chem. Soc.* **1983**, *105*, 355.
(191) Kim, S.; Jhon, M. S.; Scheraga, H. A. *J. Phys. Chem.* **1988**, *92*, 7216.
(192) González, L.; Mó, O.; Yáñez, M. *J. Chem. Phys.* **1998**, *109*, 139.
(193) Iosue, J. L.; Benoit, D. M.; Clary, D. C. *Chem. Phys. Lett.* **1999**, *301*, 275.
(194) Tarakanova, E. G. Private communication, 1996.
(195) Crooks, J.; Stace, A. J.; Whitaker, B. J. *J. Phys. Chem.* **1988**, *92*, 3554.
(196) Serrallach, A.; Meyer, R.; Günthard, H. H. *J. Mol. Spectrosc.* **1974**, *52*, 94.
(197) Bartell, L. S.; Harsanyi, L.; Valente, E. J. *J. Phys. Chem.* **1989**, *93*, 6201 and references therein.
(198) Farges, J.; de Feraudy, M. F.; Raoult, B.; Torchet, G. *Adv. Chem. Phys.* **1988**, *70*, 45.

CR990054V